Alchemical Free Energy Calculations on Membrane-Associated Proteins

Michail Papadourakis, Hryhory Sinenka, Pierre Matricon, Jérôme Hénin, Grace Brannigan, Laura Pérez-Benito, Vineet Pande, Herman van Vlijmen, Chris de Graaf, Francesca Deflorian, et al.

JCTC Journal of Chemical Theory and Computation

pubs.acs.org/JCTC
Review

Alchemical Free Energy Calculations on Membrane-Associated Proteins

Michail Papadourakis, Hryhory Sinenka, Pierre Matricon, Jérôme Hénin, Grace Brannigan, Laura Pérez-Benito, Vineet Pande, Herman van Vlijmen, Chris de Graaf, Francesca Deflorian,* Gary Tresadern,* Marco Cecchini,* and Zoe Cournia*

Cite This: J. Chem. Theory Comput. 2023, 19, 7437−7458

ABSTRACT: Membrane proteins have diverse functions within cells and are well-established drug targets. The advances in membrane protein structural biology have revealed drug and lipid binding sites on membrane proteins, while computational methods such as molecular simulations can resolve the thermodynamic basis of these interactions. Particularly, alchemical free energy calculations have shown promise in the calculation of reliable and reproducible binding free energies of protein−ligand and protein−lipid complexes in membrane-associated systems. In this review, we present an overview of representative alchemical free energy studies on G-protein-coupled receptors, ion channels, transporters as well as protein−lipid interactions, with emphasis on best practices and critical aspects of running these simulations. Additionally, we analyze challenges and successes when running alchemical free energy calculations on membrane-associated proteins. Finally, we highlight the value of alchemical free energy calculations calculations in drug discovery and their applicability in the pharmaceutical industry.

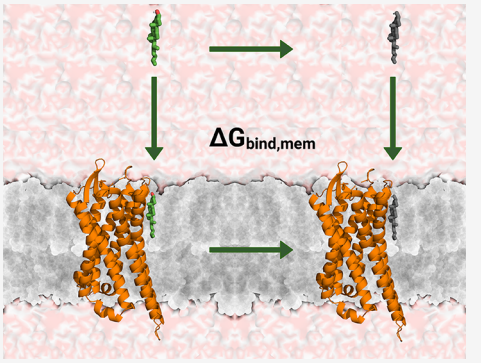

INTRODUCTION

Prediction of free energies is one of the most important applications of biomolecular simulations in drug discovery.[1,2] The ability to estimate the relative stability of different molecular states or to quantify the thermodynamic consequences of a specific mutation can provide important insights into biological systems. The basic idea behind alchemical free energy methods is to compute the difference in free energy between two states of a system, such as a protein or a ligand, as a function of a continuous transformation between the two species.[3] Such a transformation is typically accomplished by gradually altering the molecular interactions between the atoms in the system, while simultaneously monitoring the corresponding changes in free energy.[4] Alchemical binding free energy methods use a physically unrealistic (alchemical) pathway to connect states of interest. The pathway is usually known as the lambda coordinate and can vary depending on the thermodynamic cycle connecting the end states. Typically, the intermediate windows capture the transition from one molecule to another in a relative binding free energy (RBFE)[5] calculation or the progressive decoupling of a ligand in an absolute binding free energy (ABFE)[6] prediction.

Computational alchemical approaches are popular for various reasons in particular because they are more rigorous and often more accurate than end-point methods such as molecular mechanics with generalized Born and surface area solvation (MM/GBSA)[7] and are more efficient compared to full trajectory methods (e.g., Umbrella sampling,[8] Metadynamics[9]) leading to faster convergence. There are now various reports in the literature demonstrating the use of alchemical RBFE and ABFE methods for drug discovery.[10−19] The automation of the RBFE[20] and ABFE[21] pipelines has enabled their application to larger databases of compounds, including studies of hundreds and thousands of molecules.[10,16,17,22,23] The combination with machine learning techniques also offers the promise of expanding their scope.[24,25] Despite this, the computational cost is still prohibitive for large-scale virtual screening, but this is likely to change, as improved protocols and computational resources will lead to an increased impact on drug discovery. In recent years, advances in computer hardware and software have enabled more accurate and efficient calculations of alchemical free energies.[26−30] Key methods include thermodynamic integration (TI),[31] free energy perturbation (FEP),[32] and accelerated molecular dynamics (aMD).[33] In addition, nonequilibrium FEP[34,35] can

Received: March 31, 2023
Published: October 30, 2023

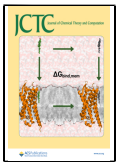

https://doi.org/10.1021/acs.jctc.3c00365
J. Chem. Theory Comput. 2023, 19, 7437−7458

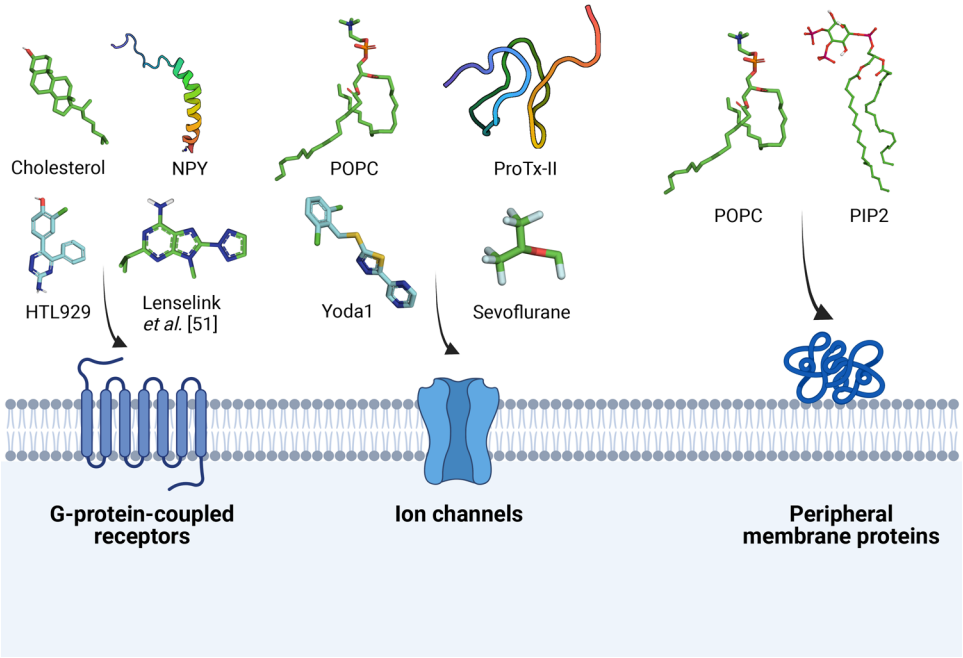

Figure 1. General overview of alchemical free energy calculations on the different classes of membrane-associated proteins that are reviewed here. It includes recent advances and challenges focusing on FEP/TI simulations of ligand, peptide, and lipid binding on GPCRs (left panel), of peptide, toxin, and ligand binding on ion channels (middle panel), and of peripheral membrane−lipid interactions (right panel).

achieve the same degree of accuracy and better convergence as equilibrium FEP calculations by performing extensive sampling only on the physical end states. These methods have been applied to a wide range of biological systems, including enzymes,[36] receptor−ligand interactions,[12,34] and protein−protein interactions.[37,38] Several recent reviews cover the basic principles, practical considerations, and applications of alchemical free energy methods, and provide a comprehensive overview of the field.[5,39,40]

Membrane-associated proteins play a critical role in cellular processes and the understanding of their thermodynamics is essential for comprehending their behavior and function.[41] Membrane proteins represent crucial drug targets because of their role in modulating cell function and signaling. For example, G-protein-coupled receptors (GPCRs) represent the largest single target family for marketed drugs with growing opportunities for structure-based drug discovery (SBDD). Membrane proteins, including GPCRs and many subfamilies of ion channels and transporters, interact with drug-like small molecules at multiple sites. Most drugs currently on the market have been designed to target the active site of proteins, also known as the orthosteric site. Allosteric ligands that bind to topographically distinct sites offer a competitive advantage over orthosteric ligands, as they are generally more selective, limit the risk of off-target effects and can be used synergistically with known drugs to potentiate or attenuate their pharmacological action.[42] Moreover, allosteric sites have been exploited to develop therapeutics for proteins that were considered undruggable.[43]

The recent advances in membrane protein structural biology, especially in the field of cryogenic electron microscopy (cryo-EM), have revealed the wide diversity of chemistry and binding sites in, for instance, GPCRs and ion channels.[44−46] The first FEP simulations of membrane proteins were used to estimate the change in dimerization affinities caused by mutations in the transmembrane helix of glycophorin A. However, these simulations modeled the lipid membrane in a simplified way, i.e. as an alkane layer.[47] The first FEP calculation featuring a membrane protein in an explicit phospholipid bilayer investigated the binding of a peptide ligand to a GPCR, the cholecystokinin-1 receptor,[48] also in the form of relative binding affinity calculations to describe mutations. One of the first studies that demonstrated the potential of absolute free energy calculations to be used in membrane-associated proteins were performed to investigate the substrate specificity of the Leucine transporter.[49] Subsequent work by Heinzelmann et al. was carried out on the binding of the substrate and ions in various configurations of the Glutamate transporter from *Pyrococcus horikoshii* using relative and absolute free energy calculations.[50] In recent years, more alchemical free energy simulations on membrane proteins have been published, with an increased total number of ligands reported in papers covering a plethora of targets. In 2016,[51] the relative binding free energy of 45 ligands against four different class A GPCRs was reported using FEP+[12]. A more detailed FEP study was performed from Deflorian et al.[52] to predict the relative binding free energies for ligands of two different GPCRs and highlighted key aspects that could lead to substantial improvements on the accuracy of alchemical free energy calculations. Finally, FEP calculations on different series of A_{2A} adenosine receptor (A_{2A}AR) agonists introduced a generalized framework, easily extensible to other GPCRs, to design ligands with tailored pharmacological properties or to predict the effects of point mutations on the basal activity of the receptors.[53]

In this review, we address the current state of the field, including recent advances and challenges of alchemical free energy calculations of pharmacologically relevant membrane-associated proteins such as GPCRs and ion channels and protein−lipid interactions (Figure 1). This review is organized as follows: first, we analyze challenges and practical aspects when running alchemical free energy calculations on

https://doi.org/10.1021/acs.jctc.3c00365
J. Chem. Theory Comput. 2023, 19, 7437−7458

membrane systems and the importance of these simulations for industrial drug discovery. Then, we discuss best practices, extending a previous report with some specifics for membrane-associated proteins. Next, recent alchemical free energy calculations on GPCRs and ion channels are reviewed with a special focus on the sensitivity of these calculations to the membrane composition, their use in virtual screening to improve docking results, and their ability to differentiate agonists and antagonists. Finally, representative FEP/TI studies to explore protein−lipid and peptide−lipid interactions are illustrated. We focus on the different strategies, software, and force-fields employed for these successful examples. We also compare results obtained from alchemical free energy calculations with relevant experimental data and with other computational techniques in terms of accuracy and computational efficiency and show their relevance for drug discovery in the pharma industry.

THEORETICAL FRAMEWORK OF USING ALCHEMICAL FREE ENERGY CALCULATIONS ON MEMBRANE SYSTEMS

Modeling Membrane Systems Creates Specific Challenges. Serious practical problems may be encountered while performing alchemical binding free energy calculations for membrane systems compared to solution calculations. Issues that should be taken into account are already mentioned in several reviews.[54−57] Important factors (not specific to the rigorous alchemical free energy calculations) include the composition of the lipid bilayer and the arrangement of the lipids on the bilayer, the protonation states of the ligand or of the protein's residues in the binding site (constant-pH simulations in membranes are especially challenging[58]), the quality of the starting structure of the system in case of the absence of high-resolution experimental structures (both in the presence of the ligand and in the apo-state, for different protein conformations), the aggregation of hydrophobic ligands in water during flooding simulations when exploring possible binding sites, etc. These factors may significantly alter the accuracy of rigorous MD calculations as they define the very system under modeling, including its correct input preparation. In addition, several key factors that are of particular interest for alchemical calculations in the membrane environment are discussed below.

The Bilayer as a Nonideal Mixture. The peculiarity of including the membrane environment in the alchemical free energy calculations is that membranes cannot be treated as a dilute solution because they are composed of multiple types of lipids with different concentrations for each lipid. Therefore, the typical solution standard state (1 M) is not directly transferable to these types of systems when computing binding free energies. For this purpose, Salari et al.[59] included the nonideality of cholesterol:POPC membranes when calculating the probability of binding of cholesterol on sites of three different GPCRs using a range of cholesterol concentrations (0−50% mol, where 50% mol is the upper limit of cholesterol concentrations in a stable lipid bilayer). This approach employed a double decoupling protocol, where a cholesterol molecule was decoupled from a series of mixed POPC/cholesterol bilayers with a cholesterol content ranging from 0 to 40% mol. The result was the estimation of cholesterol concentration−response curves for the three GPCRs, accounting for the effect of nonideal mixing in the bilayer.

Improving Convergence Using Binding Restraints. A potential source of error when FEP/TI calculations are performed concerns the convergence of the calculations. In most cases, the convergence can be improved with the introduction of well-defined restraints that limit the sampling of the decoupling process to relevant configurations.[60] However, additional challenges for the definition of these restraints are introduced when simulating the binding of a ligand or a lipid in a complex bulk such as a membrane environment. These include the distribution of the ligand across the membrane thickness and its strong orientational dependence in binding. Several studies have employed Boresch restraints[61] to restrict both the position and the orientation of the ligand in the binding site.[62,63] In addition, distance-to-bound configuration (DBC[64]) restraints have been introduced by the Brannigan and Hénin groups as part of streamlined alchemical free energy perturbation (SAFEP).[59] The DBC coordinate is used to simply and robustly define binding to sites of varying geometries, including the superficial binding sites of lipids at the protein-bilayer interfaces. SAFEP relies on flat-well restraint forces applied to DBC, which is defined as the RMSD of ligand coordinates calculated in the reference frame of the receptor's binding site. Successful application of SAFEP to free energy estimation in membranes has been reported in other studies as well.[65−68]

Inclusion of Water and Lipid Molecules. Several studies point toward the importance of correct binding site lipid/water inclusion when generating the input structures to perform reliable alchemical free energy calculations. For instance, one should be careful in using the coarse-grained (CG) MARTINI model, which can significantly reduce computational resources needed for MD simulations of large transmembrane systems,[69] in combination with all-atom (AA) MD. A recent study[66] indicated that a hybrid CG-equilibration-AA-production protocol may result in lipids being kinetically trapped in ion channel pores, despite having highly unfavorable absolute binding free energies of pore lipids (+10.0 ± 0.8 kcal/mol). This artifact was eliminated by restraining the lipids during the CG equilibration stage to allow water diffusion into the pore. In another study,[52] the authors highlighted the importance of buried water molecules in the binding site of transmembrane GPCR proteins that are not always correctly captured by automated solvation methods. When ignored, these waters can significantly deteriorate the accuracy of FEP/TI calculations.

Accounting for Charge Perturbations. Turning on or off the net charge of the simulation box during alchemical free energy calculations could also affect the accuracy of the results when using lattice-sum methods such as particle-mesh Ewald (PME[70]) for the treatment of the long-range electrostatics.[71] A charge change in PME is managed by introducing a uniform neutralizing background charge to enforce neutrality.[72] This can introduce an error in the binding free energy difference of two states with different charges, as the computed free energy will be the sum of turning on/off the charge while simultaneously turning off/on a uniform neutralizing background charge. Various schemes have been described to correct the calculated binding free energy for charge annihilation/creation effects during the decoupling of a ligand from the protein or its perturbation to a structurally similar ligand with different charge. A previously mentioned FEP/TI approach[73] proposes the simultaneous annihilation of a ligand in the binding site and the recoupling in the bulk within the same system. This strategy is also used to resolve convergence

https://doi.org/10.1021/acs.jctc.3c00365
J. Chem. Theory Comput. 2023, 19, 7437−7458

problems that arise in typical FEP/TI calculations.[74] However, one should bear in mind that this approach could be computationally demanding due to the larger size of the simulation box required. In another FEP/MD study,[68] the simulation of charged ligands with μ and κ opioid receptors introduced errors in the calculation of the binding free energy that was shown to scale as the inverse of the box length.[71,72,75] Since this error arises due to the shifting of the electrostatic potential baseline due to the use of periodic boundary conditions and PME summation, a correction on the binding free energy was applied based on Hummer et al. formula.[72] From this formula, the self-term for Ewald summation in a cubic lattice is equal to −2.837297/L, where L is the cube length. On the other hand, special correction schemes were recently analyzed for simulations involving lipid membrane systems.[76] The authors demonstrated the applicability of the coalchemical ion approach, which changes its charge at the same time that the charged ligand is decoupled from the lipid-bilayer systems, to obtain corrected binding free energies without significant finite-size errors (i.e., dependence on the dimensions of the periodic model system). They also highlighted that various modifications of the Rocklin correction[77] approach can be introduced to correct for finite size artifacts of the charged alchemical free energy calculations for lipid-bilayer systems using a continuum lipid model.[76] However, they demonstrated that there is ambiguity on whether this approach can be generalized to all lipid−protein systems.

ALCHEMICAL FREE ENERGY CALCULATIONS ON GPCRS

System Preparation Best Practices. A recent publication on the best practices for free energy benchmarks[78] discusses the details for optimal construction, preparation, and evaluation of binding free energy calculations. Although the focus of that paper was on soluble proteins, the preparation of the data set, ligands, and the protein systems also apply to membrane proteins, with the additional factor of including a membrane in the calculations, which will be discussed more in detail here.

The overarching goal of the preparation phase is to generate an input system that is stable in terms of ligand and protein root-mean-square deviation (RMSD) during MD simulations and captures the essential biophysics of the binding process. If these criteria are met, the completeness of the underlying theory (FEP, for instance) is sufficient to expect physically meaningful and accurate results. Inaccuracies then arise from only three possible causes: insufficient sampling, deficiencies in the force field, or system setup. For membrane proteins, special attention needs to be dedicated to system setup and stability due to the extra complexity. In short, membrane proteins are unstable outside the lipid environment, so the protein needs to have correct vertical positioning in the membrane, and the membrane itself needs to be well prepared and pre-equilibrated to provide a stable environment and contact around the transmembrane regions of the protein. Below we will consider the components of the system separately, but in practice, the details (e.g., the ligand formal charge, water positions, or side chain protonation states) are often interconnected.

In addition to the protein itself, the subsystem carried forward from the X-ray model into a simulation may have other components: ligand, cofactors, structural waters, other ligands (if simulating a multimer), post-translational modifications (PTMs), and excipients. The cofactors should be deliberately included or excluded based on their role in the biological activity that is being modeled; removing a cofactor from its cavity might cause unexpected movements or collapse of the cavity during the simulations. As mentioned earlier, binding of ligands to allosteric sites can often be relevant for membrane proteins. Depending on the proximity between the orthosteric and allosteric sites or the inductive or conformational effect caused by orthosteric ligand binding, it may be necessary to retain an orthosteric ligand while studying binding events at allosteric sites. For example, among several known cases in GPCRs, the agonist and allosteric ligands of the muscarinic 2 receptor are separated by just one layer of amino acids (∼7 Å).[79]

Following successful placement of ligands, careful solvation and equilibration of the system and the ligand binding pocket(s) is required. The solvation is crucial for membrane proteins for various reasons including formation of key ligand/water interactions, generally stabilizing the binding pose of the ligand, having a functional role for protein activity, and affecting protein side chain ionization states.[80] Water molecules can form hydrogen bonds with key residues in the receptor, helping to maintain the correct conformation of the protein. We will not enter into the details of protein preparation as they have been described elsewhere,[78] but side chain ionization states need special attention given the role they can play in membrane protein functional activity,[81] and in stabilizing the receptor structure.[79] Recent studies suggested that water molecules can act as proton acceptors or donors, influencing the protonation state of key residues in the receptor and modulating downstream signaling events.[82] All crystallographic water molecules can usually be retained, including structural waters close to the protein. When there are multiple crystal structures of the target protein or (highly homologous proteins) available, one should compare the different structures and identify water positions that are conserved or seen in structures of higher resolution. These water molecules can be incorporated into the system, assuming that they do not clash with the protein and ligand. Further steps are often required to ensure a complete solvation shell around the ligand and avoid trapped voids, which will not be solvated by passive diffusion from the water box during equilibration steps. Computational approaches such as WaterMap,[83] 3D-RISM,[84] or Grid-IST (GIST[85]) can be used for this purpose. In principle, the MD sampling will allow waters to arrange in equilibrium positions, but experimental and theoretical work has shown that the time scales for this can be impractically long.[86] The Grand Canonical Monte Carlo (GCMC[87−89]) water solvation technique can be useful as an automated approach to fulfill unsatisfied solvation sites. For GPCRs, special attention may be needed for internal structural waters even distal from the active site that are integral to the protein structure and functional activity. Omitting them could adversely affect the protein dynamics.[90]

In GPCRs, metal ions may play an important role and may be necessary for the system input. Several studies have shown that Na^+ modulates the affinity and activity of several GPCRs, including dopaminergic, adrenergic, and adenosine receptors.[91] These studies provided evidence for the existence of Na^+ in a defined binding site located in the helical bundle of these receptors interacting with a conserved aspartate. In more detail, the high-resolution (1.8 Å) structure of the A_{2A} adenosine receptor[92] revealed a Na^+/water cluster in the

https://doi.org/10.1021/acs.jctc.3c00365
J. Chem. Theory Comput. 2023, 19, 7437−7458

middle of the seven-transmembrane (7TM) helical bundle that was present in the inactive state of the receptor, but was found to collapse in the active state with no sodium identified.[91] Therefore, the input system for the calculations may benefit if one can recapitulate these structural details. Apart from specific structural ions, counterions are added as a standard step in system preparation to ensure overall charge neutrality.

Ligand preparation remains a crucial aspect for success, but it does not require special attention beyond what is considered for nonmembrane protein alchemical free energy calculations. The key things to consider remain the correct hydrogen and bond type assignment, the tautomeric state, the formal charge, and the force field parameters.

The membrane is another critical component. Fortunately, there are several approaches that facilitate this process, often with graphical user interfaces, to prepare an initial system with the protein embedded in a membrane with a specific lipid composition. These tools include CHARMM-GUI,[93] VMD[94] (with the Membrane plugin), PACKMOL-Memgen,[95] and commercial software such as Schrodinger Maestro.[96] The CHARMM-GUI can build the system with two different methods: insertion into a pre-equilibrated membrane or by replacement packing of lipids around the protein surface. PACKMOL-Memgen, which is built into AMBER,[97] also uses a packing algorithm and can combine lipids of different types in specific ratios. One must choose the appropriate force field parameters for the lipids, such as Lipid21,[98] Gromos54,[99] Slipids,[100] CHARMM36,[101] or Berger Lipids.[102] The force field choices need to be compatible, a viable example for working with AMBER[97] or GROMACS[103] could use the Open Force Field[104] for the ligands, the latest AMBER protein force field, and Lipid21 using PACKMOL-Memgen to construct the membrane. Ideally, membranes are built, packed, and equilibrated to reproduce experimental properties such as the area per lipid and the membrane thickness among others. The latest lipid force fields can deliver properties consistent with experiments,[105,106] but it is important to recognize that a typical free energy calculation involves orders of magnitude less simulation time than for classical MD (nanoseconds vs microseconds, respectively). Likewise, the free energy equilibration steps are likely to be substantially shorter. Therefore, one should ensure the systems are equilibrated and exhibit good stability prior to an alchemical free energy calculation. This can be done by equilibrating the protein with one of the ligands, the solvent, and the membrane complex with classical MD, and then use the equilibrated structure as input for the later alchemical free energy calculations and repeat the shorter free energy equilibration steps for each new ligand.

Free Energy Calculations to Aid GPCR Drug Discovery. In recent years, the interest in computational RBFE in drug discovery for GPCR targets has substantially increased. The validation of RBFE approaches for GPCR targets has required more effort compared to soluble proteins as reflected by numerous retrospective studies covered in the literature in contrast to prospective applications and by the limited number of GPCR targets used in published RBFE studies. One reason for it has been the limited number of high-resolution structures and also limited to class A. Early free energy calculations on GPCRs were based on homology models using the bacteriorhodopsin template.[48] Other reasons involve the challenges in GPCR modeling and the complexity of GPCR systems for free energy calculations, as covered more extensively later in this section. Similar challenges can arise for other membrane drug target families such as ion channels and transporters. Mutagenesis RBFE perturbation studies on GPCRs are not in the scope of this review; however, the technique was used to demonstrate some of the applicability, challenges, and limitations of RBFE for GPCRs and to validate GPCRs systems used for ligand binding affinity calculations. More recently, protein FEP calculations have proven useful to rationalize peptide binding, for which no structure was available. Xu et al.[107] used FEP simulations of selected mutants as part of a multidisciplinary approach to elucidate the binding mode of the native peptide agonist PYY to the human Y2 receptor. They could rationalize key interactions between the peptide and transmembrane binding site residues, leading to a detailed binding model for peptide binders to the Y2 receptor and further validation of the hY2 model based on the neurotensin receptor 1 active-like structure. Other early applications of alchemical perturbation of proteins include *in silico* mutagenesis design studies for nonalanine mutations,[108,109] validation of homology models and rationalization of ligand−protein interactions and binding modes for adenosine receptors,[110] GPR139,[111] and Cholecystokinin-1 Receptor.[48] A way to validate the applicability of RBFE calculations to GPCR targets in early investigations was to combine FEP predictions with experimental approaches or other predictive techniques. An early application relied on MD/FEP to guide fragment-based ligand discovery for adenosine receptor A_{2A}, in combination with biophysical and computational structure-based screens, and rationalization of fragment binding affinities.[112] This study showed the advantages of RBFE inclusion of protein flexibility and explicit solvent in calculating ligand binding affinities, therefore overcoming the limitation of a static binding site and the lack of water molecules in molecular docking studies. Alchemical FEP was used to elucidate structure−activity relationships (SARs) for a small congeneric series of kappa opioid receptor (KOR) antagonists in combination with virtual screening and Wscore. This was an example where FEP was used along with multiple predictive methods to estimate how ligand binding free energies can be affected by the stabilization/destabilization of water molecules in the binding site.[113] The agonist-bound and antagonist-bound crystallographic structures of β_2 adrenergic receptor (β_2-AR) were the starting systems for retrospective absolute FEP calculations with the aim of discriminating ligand efficacy for the β_2-AR inverse agonist (carazolol), the neutral antagonist (alprenolol), and the full agonist (BI-167107).[114] The authors showed how relatively short free energy calculations offer reliable physical properties to discriminate ligand efficacy, bridging between docking with static protein and highly expensive millisecond-time scale MD simulations. Finally, in a more recent study, the ligand efficacy of closely related β_2-AR compounds was also explored using RBFE calculations.[115]

RBFE calculations have gained increased confidence in driving SBDD for GPCR targets through their successful implementation on supporting the ligand binding elucidation hypothesis and through studies where they retrospectively confirmed previous experimental/computational results. There are successful examples of prospective applications to GPCR SBDD and retrospective studies probing the limits of applicability of RBFE calculation, for example for fragment-based drug design (FBDD), as described later in this section.[116,117] To challenge RBFE applicability limits, FEP calculations were applied retrospectively to extra-helical

https://doi.org/10.1021/acs.jctc.3c00365
J. Chem. Theory Comput. 2023, 19, 7437−7458

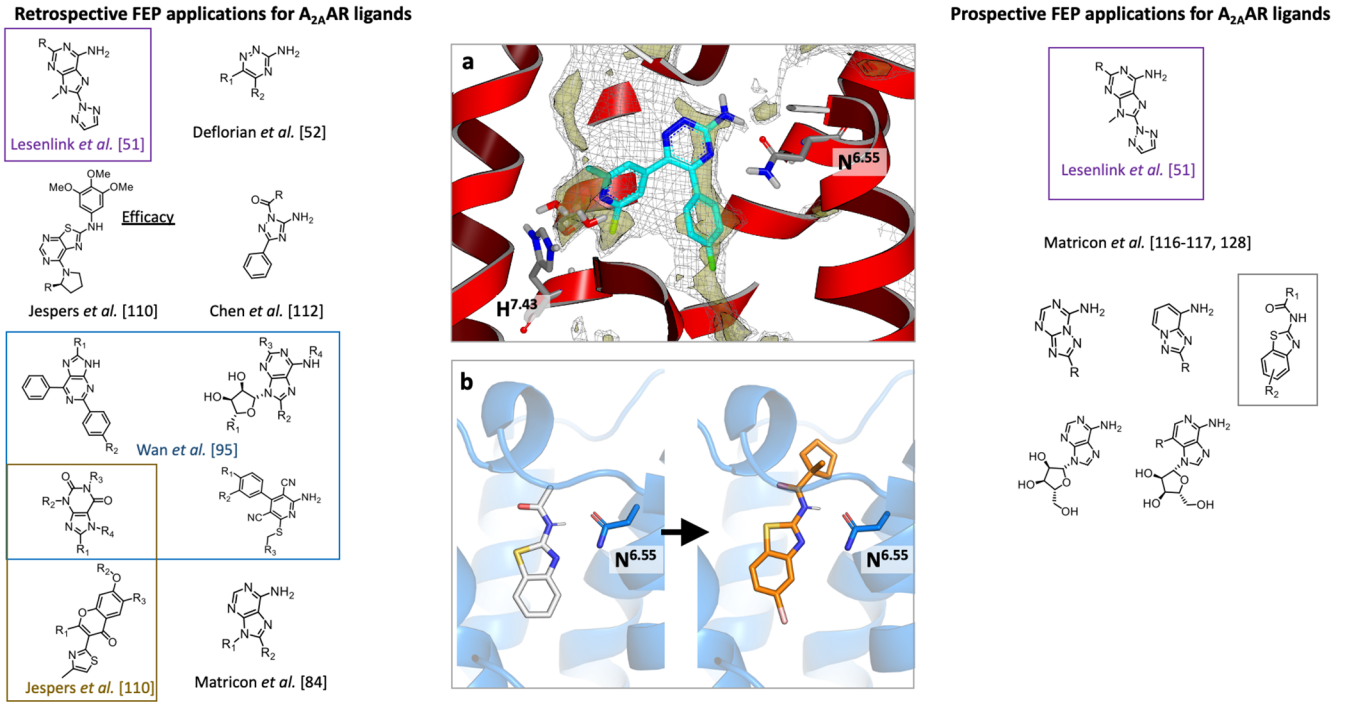

Figure 2. a. High-resolution structure of the A2A adenosine receptor ($A_{2A}AR$)in complex with AZD4635 (PDB ID 6GT3). GRID maps are shown to highlight size of the pocket (gray mesh, created using the CH3 probe in gray mesh at 1 kcal/mol) and lipophilic hotspots (yellow transparent solid surface, created with the sp2 CH probe at −2.8 kcal/mol). b. MD snapshots from application of FEP for fragment optimization at the $A_{2A}AR$ (in blue cartoon representation): initial fragment (white colored carbons) and optimized fragment (orange-colored carbons), from Matricon et al.[117] 2D structures of different A2A chemotypes investigated by RBFE calculations by authors cited in this review are shown.

binding sites. Dickson et al.[118] showed promising performance of FEP for ligand binding affinity of human P2Y1 receptor antagonists binding to a lipid-exposed, extra-helical site. The authors highlighted the challenges of using FEP to estimate ligand binding affinities for allosteric binders, where the binding site is formed by a mixed environment of protein and lipids. This retrospective study, using a small set of 30 structurally similar P2Y1 allosteric binders, showed that free energies can be calculated with an error similar to that reported for soluble targets, with a mean unsigned error (MUE) of 1.08 kcal/mol in comparison to the experimental affinities. By modifying the thermodynamic cycle and deconvoluting the observed affinity, ΔG_{obs}, into membrane affinity, ΔG_{mem}, and intrinsic affinity for the site, ΔG_{int}, contributions, this study led to the uncovering of a hydrophobic hotspot at the P2Y1 extra-helical allosteric binding site. The application of FEP to extra-helical binders highlighted the potential of RBFE calculations to optimize the intrinsic affinity. The focus on the specific activity at the target site could help to design more active molecules with optimal absorption, distribution, metabolism, and excretion (ADME) properties, as opposed to optimizing affinity for the membrane alone that would be expected to favor more lipophilic and less drug-like molecules.

The $A_{2A}AR$ is one of the best characterized GPCR from a structural perspective, and this is reflected in the amount of RBFE applications targeting this system and its close relatives A_1 and A_3 receptors. An overview of retrospective and prospective FEP studies of $A_{2A}AR$ is illustrated in Figure 2. $A_{2A}AR$ has been used as a target for multiple RBFE applications, and also to benchmark ligand binding free energy technologies, like thermodynamic integration with enhanced sampling (TIES).[119] The authors stressed that the choice of the targets, both $A_{2A}AR$ and A_1 adenosine receptor (A_1AR), was based on the availability of high-resolution X-ray structures of both active and inactive forms, as well as on experimental kinetic binding data. TIES[120] makes use of enhanced ensemble techniques to ensure reproducibility, accuracy, and precision in the calculation of relative binding free energies. The TIES application proved to be a powerful protocol for accurate prediction of RBFE between structurally similar ligands and, therefore, useful in the lead optimization stage.

As discussed in the best practices section RBFE calculations on GPCR targets are not straightforward due to modeling challenges. Confidence in the performance and applicability of RBFE calculations for GPCR targets has been built on retrospective studies,[51] mainly carried out on targets with high resolution structures and ample structural information, like $A_{2A}AR$, with small ligand sets within congeneric chemotypes and small alchemical perturbations. Those studies showed how results were target-dependent and the robustness of the performances was affected by the quality of structural data of the targets.[51] Nevertheless, the retrospective systematic validation of FEP calculations on multiple GPCRs by Lenselink et al.[51] demonstrated the applicability of the method for relatively large perturbations with performances in line with those for soluble proteins. Using $A_{2A}AR$, Lenselink et al.[51] applied FEP in a prospective fashion, identifying a highly potent antagonist with 10-fold increased potency compared to the starting compound. The study also highlighted the advantages of using different structures of the same target, retrospectively rectifying the binding energies of incorrectly overpredicted compounds. FEP calculations could be inserted into a robust workflow to iteratively evaluate receptor−ligand binding models and to prospectively drive drug design.[121]

https://doi.org/10.1021/acs.jctc.3c00365
J. Chem. Theory Comput. 2023, 19, 7437−7458

Initial binding mode hypotheses were generated based on experimental biophysical mapping data and SAR analysis and evaluated by FEP, providing structural and energetic insights into determinants of high affinity binding of the chromone derivatives, driving the prospective expansion of the chromone series.[121] Only recently, validated FEP models of GPCRs have been the basis for successful prospective drug discovery studies for A_{2A}AR.[51,116,117] Nevertheless, in contrast to soluble protein targets, no large-scale prospective applications of GPCRs have been reported.

Deep structural knowledge of the GPCR target is a crucial aspect of the success of RBFE calculations. Although the availability of high-resolution structures of GPCRs has increased, some targets are more represented than others. The applicability of RBFE calculations was also explored for targets lacking structures. Applying RBFE techniques for ligand binding affinity to GPCR homology models has proven to be challenging, and the successful cases reported in the literature show the importance of having high-confidence homology models, based on high-resolution structural templates. Cappel et al.[122] showed that FEP can be applied successfully to well-characterized homology models, like those for adenosine receptors, for which a vast structural knowledge is available due to multiple high-resolution structures of A_{2A} adenosine receptor in complex with different chemotypes. Once again, the extensive structural knowledge around A_{2A}AR makes adenosine receptors valuable targets for robust RBFE calculations from reliable GPCR homology models. Jespers et al.[110] used the well characterized A_{2A}AR and A_{2A}AR-based homology models of other adenosine receptors when experimental receptor structures were unavailable to explore various applications of MD/FEP through retrospective studies. They covered different aspects of GPCR SBDD, such as ligand binding modes, binding affinity, scaffold hopping, and agonist efficacy with the use of side chain or ligand perturbations, highlighting an applicability of RBFE calculations on homology models. The applicability of MD/FEP to distinct pharmacological classes of ligands with a focus on modality and efficacy was tested with the aim to understand the ligand mode of action by comparing the binding of each molecule to the active and inactive conformations of the receptor. An A_3 adenosine receptor (A_3AR) homology model was the target of another RBFE study to rationalize binding mode and to guide the design and structural characterization of selective antagonists of the human A_3AR.[123] Using different computational approaches, including MD and FEP simulations in conjunction with experimental approaches, the study succeeded in generating a novel series of diarylpyridine antagonists and elucidating the key role of a second nitrogen atom to stabilize a water network in the binding site.

Advantages of using RBFE approaches include the consideration of dynamic interactions between ligand and protein residues, the critical role of water molecules, and the effects on ligand binding by the perturbation and/or stabilization of water networks in the binding site. Water molecules and water networks are important in the GPCR ligand binding. The stabilization or destabilization of water molecules in the A_{2A}AR receptor binding site and the implications of water network perturbation on ligand binding have been characterized in other MD and RBFE approaches around antagonist binding.[124] An important factor in free energy calculations is how the water molecules are sampled during the simulations. Deflorian et al.[52] showed the benefits of enhancing water sampling in FEP calculations on two GPCR targets, the A_{2A}AR and orexin receptor 2 (OX2) systems. GCMC simulations were used to solvate the pocket and the entire system during FEP calculations to accelerate the sampling of the water molecules. The automated approach permits the waters to fill voids or cavities or be displaced for specific ligand perturbations. As mentioned earlier, even when performing an automated GCMC method, it is still essential to consider the explicit water structure around the ligand. If this is not done, the ligands may move to fill voids during the very first minimization stages of FEP calculations, sometimes prior to GCMC. Therefore, when water positioning and sampling are concerns, it is crucial to carefully add explicit water molecules in the binding site prior to FEP calculations and create robust and reliable water networks that are stable during system equilibration and FEP simulations. The high-resolution structures of A_{2A}AR were a decisive input for the choice of targets and the success of RBFE calculations. Water molecules as key players in ligand binding evaluation in RBFE calculations were demonstrated in the A_3AR antagonists FEP study.[123,125] FEP simulations were carried out to assess the energetics of the water-mediated interactions for ligand matched pairs[126] where the pyrimidine core was transformed to pyridine with the alchemical conversion of an N to a C−H. The drastic reduction in experimental affinity was correctly captured by FEP in agreement with the hypothesis of stabilization of the water network in the binding site by the additional pyrimidine nitrogen.[123] In follow-up work by Jandova et al.[125] the sensitivity of ligand binding affinity predictions to the charge model for the ligand core (pyrimidine vs pyridine) was further examined using TI calculations and GROMOS 54a8 force field partial charges. The authors showed how a systematic variation of the charge distribution of the ligand affected the correlation between the predicted binding affinities and the experimental data. The mean absolute error with respect to the experimental data was calculated for a small number of pyridine to pyrimidine transformations within the congeneric series, showing the optimal nitrogen charges for the best mean absolute error with respect to the experimental data. Using the optimal nitrogen charge, the authors then analyzed the enthalpic and entropic contributions to the relative binding free energies. The analysis showed that the disturbance of the water network surrounding the ligand led to the largest observed entropy decrease observed, providing insights into the binding thermodynamics of the A_3AR antagonists series.

The consideration of water networks in GPCR SBDD has also been studied with FEP approaches by Matricon et al.[116] Hydration site energetics played a central role in A_{2A}AR agonist binding. As observed in the crystallographic structures, binding of the A_{2A}AR to its endogenous agonist involves the formation of a well-defined solvent network surrounding the ligand.[127] In a particular hydration site, the loss of a hydrogen bond by replacing a nitrogen atom with a carbon atom (3-deazaadenosine) resulted in a loss of agonist potency. This effect was correctly captured by RBFEs obtained from FEP calculations, whereas several docking programs omitting hydration site energetics predicted the opposite effect. In addition, RBFEs obtained from FEP also suggested that introducing a methyl to 3-deazaadenosine would not be as favorable as replacement with a 3-hydroxymethyl, which was then confirmed experimentally.[128] Further analyses suggested that an interplay between water displacement together with

https://doi.org/10.1021/acs.jctc.3c00365
J. Chem. Theory Comput. 2023, 19, 7437−7458

ligand energetic terms both captured by FEP were essential "ingredients" to predict the enthalpy-driven relative binding effects for the designed full agonist compound.[128]

During fragment optimization, small chemical modifications can lead to complex binding thermodynamic outcomes, making this a particularly difficult application domain. Therefore, accurate RBFE calculations between a fragment hit and analogues can provide invaluable information to guide FBDD and help optimize fragments into high affinity leads. An evaluation of RBFE calculations in fragment optimization was reported by Matricon et al.[117] They studied the A_{2A}AR using a retrospective test set of 20 A_{2A}AR antagonists with known binding affinities to validate the MD/FEP protocol. Twenty fragment growing analogues were selected with RBFEs ranging from 0.0 to 3.8 kcal/mol and corresponding to alchemical transformations of one to five heavy atoms. Several crystal structures of the A_{2A}AR bound to ligands with a similar core scaffold provided an initial binding mode hypothesis for the reference fragment, highlighting again the significance of specific structural knowledge for the success of RBFE calculations and how this aspect has driven the choice of GPCR targets for alchemical binding free energy approaches. Calculated binding free energies were in strong overall agreement with experimental data (R^2 = 0.78) and within 1 kcal/mol error in most cases. In addition, the results illustrated the value of MD/FEP in guiding FBDD, as experimental binding affinities correlated poorly with differences in size/heavy atom count (R^2 = 0.10) and modestly with lipophilicity descriptors such as AlogP (R^2 = 0.44) or docking scores (R^2 = 0.42). Moreover, the study proved the crucial role of binding site solvation in fragment growing. For two molecule pairs with substantial differences in affinity, MD/FEP calculations were repeated at 13 temperatures to evaluate the temperature-dependence of the free energies and extract relative enthalpies and entropies of binding with an approach analogous to a van't Hoff analysis. The results suggested that water displacement led to opposite thermodynamic signatures depending on the nature of the pocket. Displacement of a water molecule in a rather buried and lipophilic pocket led to a gain of entropy, whereas the displacement of a water molecule in an open and polar pocket was associated with favorable enthalpy.

As mentioned, ligand orientation in GPCR FEP systems requires extreme care in order to obtain robust predictions. This care should be enhanced when dealing with fragments, as a major challenge in FBDD is fragment binding mode promiscuity.[129] Matricon et al.[117] designed alchemical transformations enabling FEP calculations between two possible binding modes and demonstrated how MD/FEP transformations can be used to investigate possible fragment binding modes and tackle a major challenge in FBDD. Encouraged by the retrospective study, Matricon et al.[117] applied the same FEP approach to prospectively discriminate 12 fragments within three series. The direction of the binding free energies was correctly predicted in most cases. For two incorrectly predicted compounds, analysis of force field torsional profiles in comparison with density functional theory (DFT) data showed that the corresponding substituents were associated with substantially high and narrow torsional barriers with incorrect minima, resulting in an incorrect sampling of binding modes in favor of the weakest reference fragment in terms of free energies. Reparametrization of torsional terms led to rectified FEP predictions showcasing how critical it can be to perform force field quality checks prior to FEP calculations. Moreover, some predictions could be further improved by increasing the amount of sampling, which allowed binding mode adjustment through the opening of a salt bridge located in the extracellular vestibule (as observed in several A_{2A}AR crystal structures).

In a follow-up study, Matricon et al.[116] applied FEP to guide fragment growing with a focus on subtype selectivity, another challenge of FBDD, with the aim to reduce off-target effects. The authors investigated whether potency and selectivity could be achieved at the A_1 subtype by fragment growing into a subpocket with an amino acid difference between the subtypes. An initial prospective set of nine compounds with substituents of different sizes was used for the FEP calculations. Three compounds had a nanomolar affinity at the A_1AR but without any substantial subtype selectivity. A subsequent introduction of additional substituents, predicted to reach deeper in the orthosteric pocket, was used for FEP versus both ARs subtypes to guide fragment growing, both in terms of potency and subtype selectivity at the A_1AR. The FEP calculations led to the discovery of compound **9** with a remarkable 10 nM affinity (>1000-fold increase with respect to the initial fragment) and 38-fold subtype selectivity at the A_1AR. Analysis of MD simulations showed that targeting a residue difference in a nonburied subpocket was initially not sufficient to achieve subtype selectivity, possibly due to fragment binding mode rearrangements. Furthermore, it was observed that additional substituents deep in the orthosteric pocket were required to improve selectivity against A_{2A}AR. Overall, a robust performance of FEP was achieved to guide potency (ρ = 0.80, MUE = 1.1 kcal/mol, for 24 perturbations) and subtype selectivity (ρ = 0.85, MUE = 0.5 kcal/mol, for 15 perturbations) for the A_1AR.

ALCHEMICAL FREE ENERGY CALCULATIONS ON ION CHANNELS

Ion channels are pore-forming proteins that allow the flow of ions across lipid membranes by opening and closing in response to external stimuli as diverse as ligand binding, changes in the electrical transmembrane potential, or mechanical stress in the lipid bilayer. The illumination of ion channel structures with atomic resolution, starting with K^+ channels and, most recently, ligand-gated ion channels, has greatly improved our understanding of the molecular mechanisms underlying ion channel function. Currently, ion channels represent the second largest target for existing drugs after GPCRs. As of today, several reviews devoted to the computational studies of ion channels have been reported.[54−57,130,131] Here, we focus on the recent implementations of rigorous binding free energy calculations based on alchemical free energy approaches (FEP and TI) for the calculations of ligand-binding affinities (ΔG_{bind}) in ion-channel proteins, and their relevance to computational drug design.[132] Within the scope of this review, we will focus on the studies in which the surrounding lipid bilayer was explicitly modeled. Although protein−lipid interactions are relevant for the pharmacology of ion-channel proteins, this topic will be considered in the next section.

One of the first applications of absolute binding free energy calculations in ion channels focused on the interaction of general anesthetics with the nicotinic acetylcholine receptor[133,134] and the bacterial homologue GLIC.[135] Although the algorithms and the computational power available at that time made convergence quite challenging, the predictions by LeBard et al.[135] were confirmed experimentally shortly

https://doi.org/10.1021/acs.jctc.3c00365
J. Chem. Theory Comput. 2023, 19, 7437−7458

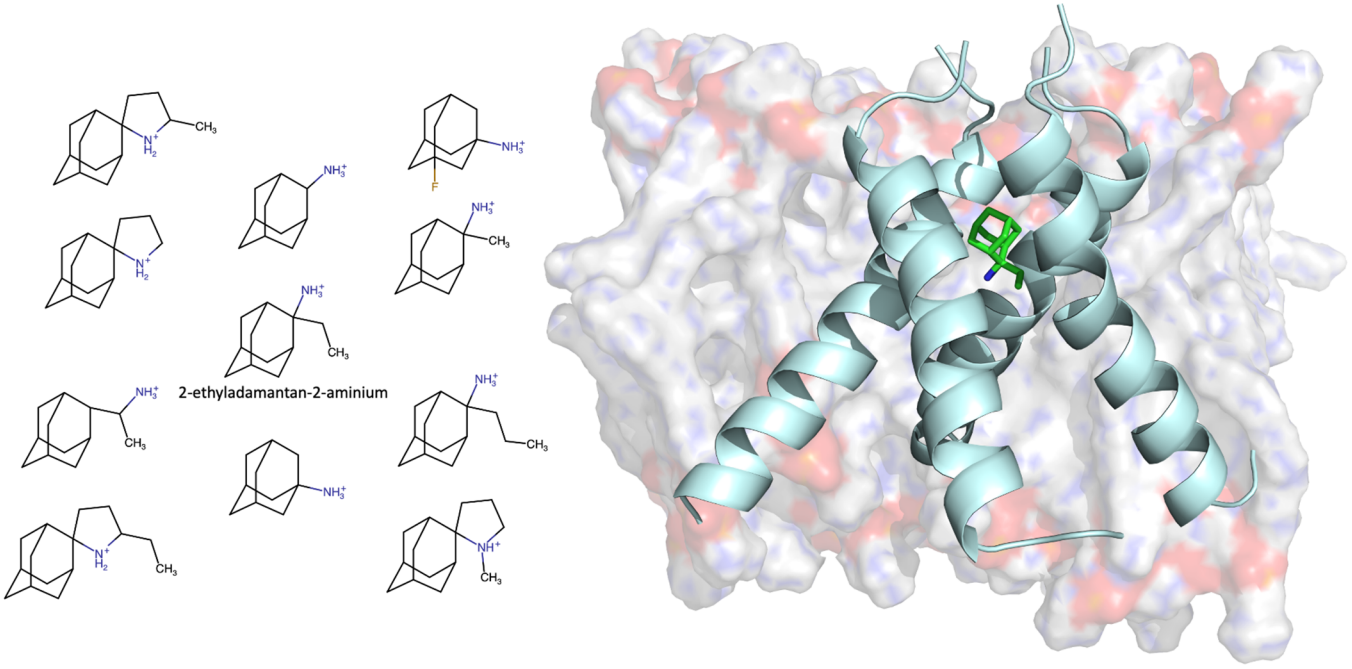

Figure 3. Binding site of aminoadamantane derivatives, pore blockers, bound to the transmembrane domain of wildtype influenza A M2 proton channel (M2TM) in its opened state (Protein Data Bank structure 3C9J[140]). On the left, examples of ligands from aminoadamantane congeneric series that were explored in a previous study are shown[137] using FEP to calculate the difference in their free energy of binging to M2TM with respect to amantadine. On the right, an amantadine analogue is shown bound to M2TM embedded in a DPPC model membrane. The correlation of FEP-calculated relative free energies of binding compared to the experimental results showed a $R^2 \approx 0.85$.

afterward,[136] demonstrating the predictive power of the approach even in its early form. On the other hand, the lack of structural information at a high resolution, e.g., for the nicotinic acetylcholine receptor, as well as the absence of a quantitative comparison with experiments make those early attempts difficult to interpret. Another early application of alchemical FEP is the work of Gkeka et al.[137] In this study, RBFE calculations were used to predict the binding affinity of 11 aminoadamantane channel blockers of the M2 membrane protein of the influenza A virus (Figure 3). The comparison between experimental and calculated ΔG_{bind} showed a remarkable R^2 of ≈0.85, which highlights the pharmacological relevance of these calculations. Interestingly, in the absence of lipids, R^2 dropped to ≈0.20, thus demonstrating the importance of an explicit representation of the membrane environment for accurate binding affinity predictions. Similar conclusions were reached in a subsequent study on the same system, where the correlation between FEP-calculated and experimental ΔG_{bind} was shown to deteriorate when moving from 1,2-dimyristoyl-*sn*-glycerl-3-phosphocholine (DMPC) (R^2 = 0.88) to 1,2-dipalmitoyl-*sn*-glycero-3-phosphocholine (DPPC) (R^2 = 0.56) lipids, albeit with a root-mean-square error (RMSE) below 1 kcal/mol in both cases.[138] In addition, it was discussed that the poorer performance of FEP calculations for a mutant of the M2 protein (R^2 = 0.24) was possibly due to the absence of high-resolution structures for the mutant. As more structures emerged, rigorous binding free energy calculations played a greater role in untangling the complexities of anesthetic pharmacology. For instance, later studies involving absolute binding affinity calculations of propofol to four pseudosymmetric sites in the GABA(A) receptor yielded insights into the origins of the subunit selectivity that contributes to tissue dependent response.[139]

In a more recent study, molecular docking and ABFE calculations were used to predict the binding affinities for 12 small inhibitors of the voltage-gated potassium channel hERG.[141] It was shown that although the docking results were poorly correlated with the experiments ($R^2 \approx 0.26$), the correlation could be greatly improved by the rigorous binding free energy calculations ($R^2 \approx 0.77$), reaching an impressive $R^2 \approx 0.91$ after refinement of the initial docking poses for two ligands. Last, when the performances of the methodology were evaluated prospectively using a regression model, an RMSE of 0.73 kcal/mol from experiments was obtained, which is below the chemical accuracy limit.[141] Most recently, ABFE calculations in combination with replica exchange molecular dynamics (ABFE/REMD) were used to predict the binding affinity of a potent agonist (Yoda1) and one antagonist (Dooku) of the mechanosensitive channel Piezo1 in both the open and closed states of the channel.[142] Insightfully, it was found that the differential binding affinity of the ligand for the open versus the closed state of the channel is able to discriminate between agonists and antagonists as predicted by the Monod−Wyman−Changeux (MWC) model.[132] In addition, it was shown that an analysis of the $\Delta\Delta G$ of binding (i.e., open versus closed) for seven analogues of Yoda1 by RBFE calculations yields chemical insights on the gain or loss of agonistic activity in agreement with efficacy data from the literature. The reported accuracy (<1 kcal/mol) and the potential throughput via RBFE calculations make the design of mechanosensitive channel agonists and antagonists within reach.

Another area of active research for free energy calculations involves the prediction of the strength of ion channel/peptide interactions, including natural toxins, which provide alternative pharmacological approaches. Earlier work on the effects of mutation on the binding affinity of marine toxins to the

https://doi.org/10.1021/acs.jctc.3c00365
J. Chem. Theory Comput. 2023, 19, 7437−7458

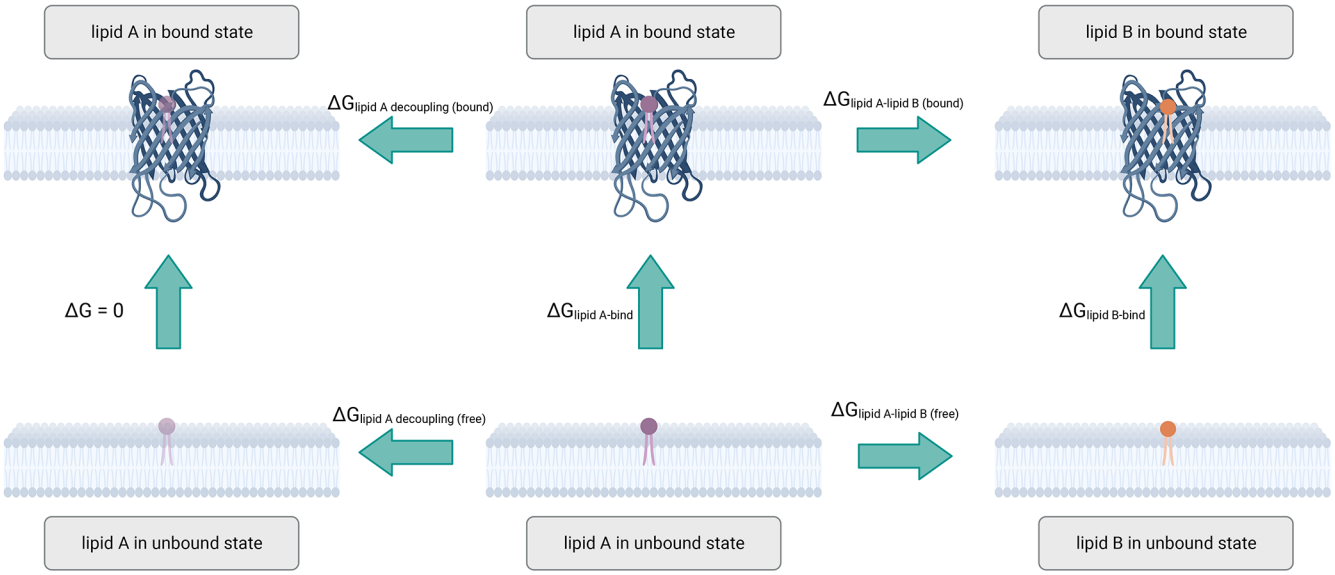

Figure 4. Thermodynamic cycles for ABFE and RBFE calculations in the case of protein−lipid binding. On the left cycle, a lipid molecule (lipid A) is fully removed from the system, while in the right cycle, lipid A is transformed into a structurally similar lipid molecule (lipid B). Both transformations occur in the bound state (upper panel) and the unbound state (lower panel). The protein receptor is shown as a beta-barrel, while lipid A and lipid B are depicted as magenta and orange phospholipids, respectively.

voltage-gated potassium channels Kv1.1 and Kv1.3 showed predictions within chemical accuracy when using alchemical approaches (TI or FEP).[73,143] Recently, the affinity of 47 point mutants of gating-modifier toxins at the voltage-gated sodium channel Nav1.7 was investigated by RBFE calculations based on alchemical FEP and recent cryo-EM structures for the development of nonopioid analgesics.[144] The FEP calculations predicted relative potencies with an RMSE of 1.0 kcal/mol and an R^2 value of 0.66, which outperformed end-point free energy results based on MM/GBSA (RMSE ≈ 3.89 kcal/mol and R^2 ≈ 0.56). Moreover, by combining MM/GBSA with FEP, an efficient workflow for the rapid screening of hundreds of toxins' mutations was implemented and used to identify 15 nonstandard tryptophan mutants at Protoxin-II with a predicted gain in potency greater than1 kcal/mol.[144]

In addition to the above approaches, rigorous binding free energy calculations in ion channels were recently used as a tool to characterize allosteric binding sites, predict the tautomeric form of ligands bound to proteins, or support the physiological relevance of structural models extracted from MD simulations. In a recent study, the binding affinities of two tautomers of 2-guanidinobenzimidazole to five mutants of the Hv1 voltage-gated proton channel were explored by RBFE calculations via alchemical FEP.[145] The mean absolute error (MAE) of 1.1 kcal/mol obtained with one of the tautomers indicates the preferred tautomeric form of this prototypical channel blocker when bound to the ion pore and provides support to the open state model of the human Hv1 channel generated by multi microsecond MD simulations started from the closed state and with voltage applied.[146] In other studies on the M2 proton channel of influenza A, RBFE calculations were used to investigate the change in the affinity of (*R*)- versus (*S*)-enantiomers of the anti-influenza drug rimantadine.[147,148] In agreement with electrophysiology kinetic assays, the FEP results showed no difference in binding affinity, supporting the conclusion that the chirality of drugs binding the M2 proton channel has no effect on binding or channel inhibition despite the M2 pore being chiral. In another investigation on the proton channel M2, absolute FEP calculations were used to predict the binding site of an aminoadamantane derivative known to produce strong inhibition against influenza virus A *in vitro*.[149] The computational predictions validated on two experimentally characterized protein mutants suggest that this aminoadamantane derivative deeply penetrates the M2 channel pore strengthening the hypothesis that its antiviral effect derives from an open-channel block.[149] The same approach was used to refine docking poses of the general anesthetic sevofluorane on the voltage-gated potassium channel Kv1.2 and obtain a 3D map highlighting the complexity of molecular recognition at membrane receptors with multiple binding sites with single or multiple occupancy states being in competition.[150,151] Last, both absolute and relative FEP calculations in ion channels were used to assign ambiguous disconnected electron densities in protein crystal structures. In the case of the fluoride channel Fluc, for instance, the higher affinities of water molecules relative to fluorine ions were demonstrated at several sites, regardless of previous speculations.[152]

ALCHEMICAL FREE ENERGY CALCULATIONS OF PROTEIN−LIPID AND PEPTIDE−LIPID BINDING IN MEMBRANES

Membrane proteins can interact with multiple lipid species and these interactions influence the function of the proteins either directly[153−155] or allosterically.[156,157] The nature of these interactions can be analyzed by using free energy calculations. In the following section, computational studies focusing on protein−peptide−lipid interactions will be presented.

Using free energy calculations for protein−lipid interactions dates back to 2008 when FEP and TI calculations using the BLOCK module in CHARMM[158−160] were performed to study the free energy of binding of the prothrombin fragment 1 (PT1) in the presence of Ca^{2+} to a mixed membrane that contains phosphatidylserine (PS) and phosphatidylcholine (PC) relative to a membrane that contains only PC.[161] This

https://doi.org/10.1021/acs.jctc.3c00365
J. Chem. Theory Comput. 2023, 19, 7437−7458

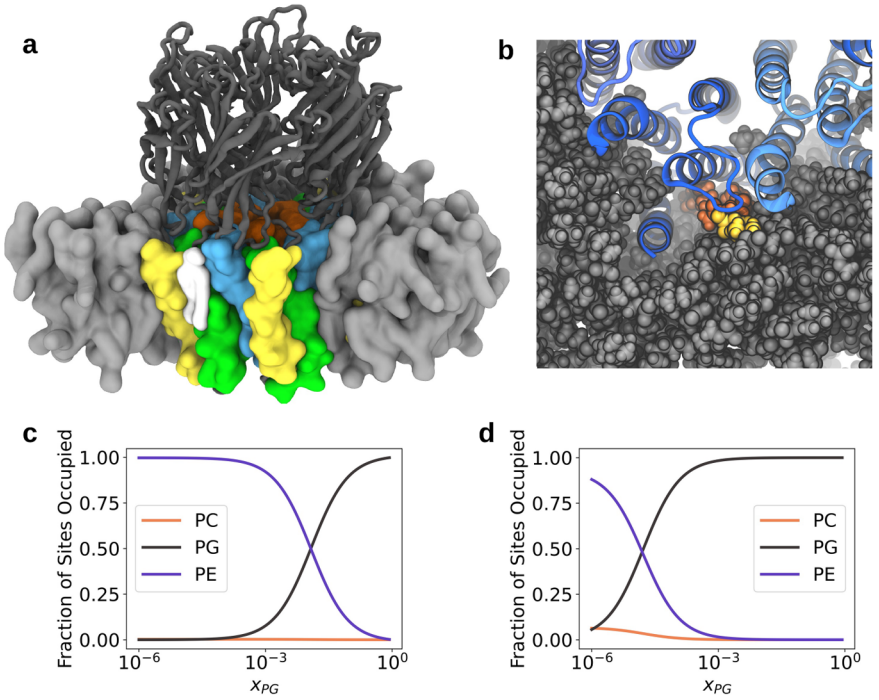

Figure 5. Prediction of state-dependent selective lipid binding by the ELIC ligand-gated ion channel using SAFEP. (a) Rendering of ELIC (dark gray extracellular domain, cyan helix M1, red M2, green M3, yellow M4) in a lipid bilayer (gray) with a bound phospholipid (white). (b) Alchemical transformation of the headgroup of a POPC lipid (red) bound to ELIC (blue cartoon) into a PG headgroup (yellow) in a POPC bilayer (gray). (c) Computational titration curves predicting the occupancy of the binding site by PC, PE, and PG for the wild-type receptor in a nonconducting conformation. (d) Similar lipid titration curves for the ELIC5 mutant in an open-pore conformation.

study observed a difference in the binding free energy of the PT1-Ca^{2+} complex when using different binding sites of the protein. Particularly, the free energy of binding of the PT1-Ca^{2+} complex on site 1 was equal to −11.5 kcal/mol, while that on the second site was estimated to be around −8.8 kcal/mol. Protein−lipid interactions were also investigated using potential of mean force (PMF) calculations, FEP and well-tempered metadynamics with the MARTINI force-field[162] to study both bacterial and mammalian membrane protein−lipid systems.[65] This work concluded that all three techniques provide a similar degree of accuracy with predicting binding free energies of the four experimentally well-characterized membrane proteins converging to values within the standard deviation of the methods. The computational efficiency of the three techniques was compared with FEP being the least computationally demanding technique (five independent repeats resulting in ∼25−40 μs total simulation time) compared to PMF (∼50−75 μs) and well-tempered metadynamics (∼120−190 μs). Finally, this work provided an automated implementation of these techniques so that they can be exploited for newly determined membrane protein structures. Elber and co-workers employed FEP calculations to investigate the impact of phosphatidylinositol 4,5-bisphosphate (PIP2) protonation on its binding to transient receptor potential vanilloid 5 (TRPV5).[163] The results suggest that PIP2 is in a deprotonated state in the binding site. More recent examples using FEP calculations investigated the strength of the phosphatidylinositol 3,4,5-triphosphate (PIP3) binding to the C-terminal FYVE domain of Early Endosome Antigen 1 (EEA1) protein,[164] the interaction of PIP2 with six Ca^{2+}-independent C2 domains from kidney/brain protein (KIBRA), phosphatidylinositol 4-phosphate 3-kinase C2 domain-containing subunit α (PI3KC2α), RIM2, phosphatase and tensin homologue (PTEN), SH2-containing 5′-inositol phosphatase 2 (SHIP2), and SMAD-specific E3 ubiquitin-protein ligase 2 (Smurf2).[165] The free energies for converting PIP3 or PIP2 to PC showed a more favorable binding of PIP3/PIP2 compared to PC to the proteins of interest. Finally, phosphatidylinositol (PIP) and PIP3 showed weaker binding to the transmembrane domain of Polycystin-2 (PC2)[166] based on CG FEP calculations ($\Delta\Delta G_{PIP2\rightarrow PIP}$ = 21.0 kJ/mol and $\Delta\Delta G_{PIP2\rightarrow PIP3}$ = 4.0 kJ/mol). These studies followed the same approach regarding the FEP calculations: the target lipid molecule is transformed *in silico* into a generic lipid or fully removed from the system.[167] This approach is depicted on Figure 4 and it was also applied to compute the binding free energy of different phospholipids to the human inward rectifying potassium 6.2 (hKir6.2) channel.[168] This work demonstrated a good agreement between the direct perturbation ($\Delta\Delta G_{PIP2\rightarrow PC}$ = 33 ± 3 kJ/mol) and the multistep perturbation ($\Delta\Delta G_{PIP2\rightarrow PI4P\rightarrow PI\rightarrow PC}$ = 30 ± 1 kJ/mol) of PIP2 to PC. Following the same approach, FEP calculations were performed to examine the affinity of different anionic phospholipids in the PIP2 binding site of TWIK related K^+ channel 1 (TREK1).[169] It was shown that the different lipids bind more favorably to the same conformational state of TREK1 (up state) compared with the other conformational state (down state). Another study from the Sansom group compared the PIP2 over PS binding to two experimentally determined sites of the Kir2.2 channel[170] using FEP calculations. The results highlighted a strong preference for PIP2 over PS in both sites (43.2 ± 1.2 kJ/mol for the primary site and 29.4 ± 1.7 kJ/mol for the secondary site). FEP calculations were also performed on the *Saccharomyces*

https://doi.org/10.1021/acs.jctc.3c00365
J. Chem. Theory Comput. 2023, 19, 7437−7458

cerevisiae supercomplex structure containing Complex III (CIII) and Complex IV (CIV) to study its interaction with cardiolipin (CL) and monolysocardiolipin (MLCL).[171] It was shown that CL binds more favorably to the complex compared to MLCL with a $\Delta\Delta G$ value of 8 kJ/mol, due to its interactions with CIV. In another work, FEP calculations were performed to investigate ceramide's inhibitory activity at open and closed states of the hERG1 channel.[172] Ceramide showed a ca. 19.6 kJ/mol higher affinity for the closed state compared to the open state. Moreover, absolute FEP/λ replica-exchange MD simulations in NAMD2.14[173] were employed to study the energetic stability of POPC lipids inside the pore domain of the mechanosensitive Piezo1 channel in a nonconducting conformation.[66] The absolute binding free energy of the lipids in the Piezo1 pore corresponds to the free energy difference between lipids in the pore and lipids in a homogeneous POPC bilayer. The results indicated that one full lipid in the pore exhibits an unfavorable binding free energy (+41.8 ± 3.3 kJ/mol). In recent studies by Waheed et al., the free energy cost of alanine substitution of aromatic residues in peripheral membrane proteins[174] and phosphatidylinositol-specific phospholipase C (PI-PLC) enzymes[175] was computed. This was performed to examine the contribution of the cation-π interactions of the aromatic residues with choline-containing lipids in peripheral membrane protein affinity. Finally, streamlined Alchemical FEP (SAFEP) calculations with the atomistic CHARMM36 force field have been performed to calculate the binding free energies of cholesterol with different GPCRs.[59] The results obtained from the μ-opioid (ca. −12 kJ/mol) and 5-HT_{2B} (ca. −18 kJ/mol) receptors were in line with energies obtained from other calculations, whereas the binding of cholesterol to the β_2-adrenergic receptor (ca. −53 kJ/mol) was predicted to be much stronger compared to that of other techniques. The same approach was used to study the positive allosteric modulation of Erwinia ligand-gated ion channel (ELIC) by a 1-palmitoyl-2-oleoyl-*sn*-glycero-3-phosphoglycerol (POPG) lipid:[67] it was shown that POPG has preferential binding (free energy values ranging between −17 and −24 kcal/mol) on both WT agonist-bound (preactive state) and ELIC5 agonist-bound (open state) structures compared to the other two lipids, 1-palmitoy-2-loleoyl-*sn*-glycero-3-phosphocholine (POPC) and 1-palmitoyl-2-oleoyl-phosphatidylethanolamine (POPE) (Figure 5). This finding agreed with activity measurements using a fluorescence stopped-flow liposomal flux assay.

Peptide binding to membrane bilayers has been studied by different groups over the years. FEP calculations were carried out to calculate the effective pK_a of an arginine side chain as a function of its location in a DPPC lipid bilayer[176] as well as membrane composition (DPPC, SDPC, and SDPC/SDPE mixtures with 0, 20, and 40% cholesterol).[177] Based on the results, arginine adopts a protonated form in a DPPC bilayer (predicted pK_α is 7.7 ± 0.7) and shows narrower pK_a shifts compared to SDPC and SDPC/SDPE mixtures. Finally, the presence of cholesterol stabilizes the neutral state. The interactions of Caveolin-1 (cav-1) peptides with cholesterol-rich, cholesterol-depleted and unsaturated lipid membrane systems were explored using TI calculations with the CG MARTINI model.[178] It was shown that the binding of cav-1 is more favorable to cholesterol-rich bilayers by examining the difference in the free energy of partitioning between POPC and POPC-cholesterol bilayers (about 140 kJ/mol) and between DPPC and DPCC-cholesterol bilayers (about 100 kJ/mol). Zhang et al. also explored the use of FEP calculations with an implicit membrane/solvent model (generalized Born with a simple switching function (GBSW) in combination with the Gouy−Chapman−Stern (GCS) model for a charged interface) for the computation of membrane binding free energy of peptides and proteins to an anionic membrane.[179] Test calculations on a series of peptides predicted binding affinities in close agreement with the experimental data (less than 2 kcal/mol in most cases). In addition, TI calculations were performed to calculate the partition free energies of WALP peptides that form α-helical transmembrane domains between a liquid-ordered (Lo) and liquid-disordered (Ld) phase of heterogeneous model membranes.[180] All of the peptides demonstrated a strong preference for the Ld phase. Finally, Brewer and Zhang predicted a stable binding structure of the cationic peptide human β defensin type 3 (hBD-3) on a POPG lipid bilayer and they used FEP calculations to predict the binding free energy of each amino acid by mutating it into alanine.[181] This study highlighted the importance of the tail region in the antimicrobial activity of the peptide, which was also supported by experimental findings.

An important aspect of protein−lipid interactions is the accurate prediction of the free energy cost of membrane-protein insertion. To this end, FEP calculations were performed to measure the free energy of transfer from the translocon to the membrane for arginine and leucine amino acids carried by a background polyleucine helix.[182] The theoretical estimates demonstrated an improved agreement with the experimental translocon scale compared with prior computational investigations. A similar approach was also performed to predict the membrane-insertion free energy of the wild-type outer membrane phospholipase A (OmpLA) and the mutants A210R, A210S and A210L using three aqueous reference states: fully folded protein, seven-residue strand (residues 207−213) and a single isolated residue.[183] This study demonstrated that FEP calculations agree with experiments only under certain conditions for each mutation. Dubey et al. employed free energy calculations using the MARTINI forcefield to predict the free energy of insertion of individual beads, model peptides composed of a single representative bead type and finally polyalanine peptides of increasing lengths to a DPCC membrane.[184] It was shown that the charged moieties have the least favorable free energy of insertion and that there was a nonlinear length dependence of polyalanine peptides with the lipid-mediated component.

Applications of RBFE to Other Membrane Protein Families. The use of FEP/TI has found applicability in other domains of membrane-associated systems such as calculations to study antimicrobial peptides binding to outer membrane bacterial receptors.[63] In this study, the free energy of binding (−8.89 kcal/mol) obtained from FEP calculations of the antimicrobial peptide microcin J25 was in close agreement with the experimentally determined value of −8.13 kcal/mol. In another study, alchemical free energy calculations were applied to examine the energetics of dopamine (DA) translocation through the human DA transporter (hDAT). The computed extracellular binding free energy (−7.8 ± 1.5 kcal/mol) of DA to the outward-facing hDAT was in close agreement with the experimental value (−7.4 kcal/mol).[185] In addition, FEP calculations for several inward-facing hDAT states shed light on the facilitation of the DA intracellular release by cotransported ions, with DA binding affinities decreasing with the increase of Na^+ numbers in the binding

https://doi.org/10.1021/acs.jctc.3c00365
J. Chem. Theory Comput. 2023, 19, 7437−7458

site.[185] FEP calculations were also employed to predict the binding free energy of the antimalarial drug atovaquone to the cytochrome bc_1 complex, including the effect of two specific mutations.[186] However, due to the complexity of the system, FEP simulations were not able to draw a clear conclusion on the mutations' effect on the binding free energy of atovaquone. Ion selectivity in both the inward-open and outward-open states of the electroneutral antiporter Nhap1 of *Methanocaldococcus jannaschii* (MjNhaP1) was examined using free energy calculations.[187] The differences in the ion-binding free energies of Na^+ ($\lambda = 0$) and K^+ ($\lambda = 1$) in both inward-open (ΔG^{In} = 5.2 ± 0.3 kcal/mol) and outward-open (ΔG^{Out} = 0.4 ± 0.1 kcal/mol) suggested that MjNhaP1 is selective for Na^+ over K^+. FEP calculations implemented in the Schrodinger suite (FEP+) were used to investigate how the F- to Br-substitution affects the paroxetine binding free energy to the serotonin transporter (SERT).[188] The alchemical perturbation from F- to Br- is energetically favorable in both ABC ($\Delta\Delta G = -1.63 \pm 0.39$ kcal/mol) and ACB ($\Delta\Delta G = -1.08 \pm 0.57$ kcal/mol) poses of the SERT likely due to favorable enthalpic contributions between the Br- and the negatively charged oxygens of nearby residues. Finally, both absolute and relative FEP calculations were applied to the same target to reveal the binding pose of a known allosteric inhibitor and the SAR of its analogues to the same binding site.[189]

DISCUSSION

Alchemical free energy calculations have shown promise in the calculation of reliable and reproducible binding free energies in membrane-associated systems, such as G-protein-coupled receptors (GPCRs), ion channels, transporters, as well as protein−lipid interactions, with a particular focus on drug design applications.

The increasing number of studies reporting binding free energy calculations applied to GPCRs, retrospectively and prospectively, is clear evidence of the growing value of alchemical free energy methods for GPCR drug discovery. Recent advances improved the speed and accuracy of RBFE calculations; however, such applications are relatively few compared to soluble proteins and use smaller ligand sets. Rigorous RBFE calculations remain a challenge to apply routinely in GPCR SBDD. The most time-consuming and human-demanding stage is the setup of the system and the validation of the models. A critical step for GPCRs is to generate viable starting molecular systems that are essential for obtaining reliable RBFE predictions. As described in the best practices section, this first stage involves the careful preparation of the receptor prior to running free energy simulations with particular care for the ligand and the binding site. Typically, RBFE simulation times are insufficient to rectify incorrect side chain assignments, buried waters, or incorrect ligand binding poses.[5] Moreover, when RBFE calculations are carried out with fully solvated membrane-embedded systems special attention needs to be paid to establishing the stability of the system during classical MD simulations prior to alchemical studies.[52] Often each system requires bespoke and arduous treatments, including thoughtful analysis of rotameric, tautomeric, and ionization states of protein side chains and optimization of water networks in the binding site to avoid kinetically trapped water molecules. Different features and tools of FEP calculations need to be assessed and validated retrospectively before being used for prospective drug design. Key tools are water placement methods such as those mentioned above (for example, WaterMap, 3D-RISM, GIST) to identify stable water locations in the binding site. Next, tools or additional tactics, such as GCMC water placement and sampling, extended system sampling, extended equilibrations, and replica exchange, can all be considered. Once retrospectively validated, GPCR systems have shown successful primary applications of RBFE in predicting relative ligand binding affinity for diverse GPCRs, including FEP methods to aid FBDD. With the increase in GPCR structural knowledge available by X-ray and cryo-EM, we anticipate an increase in rigorous free energy methods to aid GPCR SBDD. Nevertheless, we acknowledge that other highly desired applications of alchemical methods, already applied for soluble proteins (e.g., ABFE to rescore virtual screening hits), might take longer to be performed on GPCRs.

Recent alchemical binding free energy calculations in ion channel proteins demonstrated significant correlations with experiments and with mean errors below the limit of chemical accuracy (<1 kcal/mol) for several protein systems relevant to drug design. Importantly, both absolute and relative FEP/TI calculations have been used to gather evidence that calculated binding affinity differences are useful to discriminate agonists from antagonists retrospectively, which opens up the rational design of inhibitors and activators of ion-channel proteins.[142] In addition, several recent examples of accurate protein−peptide binding affinity predictions via alchemical free energy methods offer the perspective of rational drug discovery at synaptic receptors and sensors via site-directed mutagenesis of natural toxins from plants or animal venoms. Lastly, alchemical calculations in ion channel proteins were shown to be a broadly useful tool in drug discovery, e.g., ranking the most probable binding sites or predicting the tautomeric form of ligands bound to the ion channel. The discussed works emphasize the need for an explicit treatment of the membrane to obtain adequate accuracy, as well as the sensitivity of the free energy results on membrane composition. Other known factors such as the absence of high-resolution structures of the target or the lack of a proper parametrization of the force field, which are not specific to membrane proteins or ion channels, may limit the predictive power of alchemical calculations. At the same time, a significant improvement of the alchemical free energy predictions over docking or end-point methods was reported in several studies focusing on ion channels and GPCRs. This indicates that rigorous free energy methods are often accurate, although computationally intensive, and may be impactful tools in drug discovery.

FEP/TI calculations studying protein−lipid interactions are mainly conducted by mutating the target lipid molecule into a generic lipid or fully removing it from the system. In most of the studies presented in this review, a PIP2 or PIP3 lipid was transformed into a POPC molecule using the Martini CG force-field. Computational cost can be reduced further, as solvent and complex FEP calculations can be performed in the same simulation box, with the bound lipid in one membrane leaflet and the free lipid in the other. In addition, determination of protein−lipid interactions using FEP, PMF, and well-tempered metadynamics methods on integral membrane proteins, suggested that FEP can produce robust estimates while requiring less computational time.[65] However, prior identification of a single lipid site is required for FEP to provide insights into protein/lipid interactions. To this end, FEP/TI calculations have been performed for several protein membrane systems, and the obtained energies were in line with

https://doi.org/10.1021/acs.jctc.3c00365
J. Chem. Theory Comput. 2023, 19, 7437−7458

experimental assays. In particular, for peripheral membrane proteins (PMPs), FEP outperform PMF calculations in terms of computational cost as the length of a PMF reaction coordinate for a PMP can be up to 4−5 nm, and thus, achievement of convergence is difficult due to the slow rotation of the PMP. Finally, FEP/TI calculations were also employed by different groups to study peptide binding to membrane bilayers as well as the free energy cost required for protein−membrane insertion. In these studies, a different perturbation strategy was followed, where the residues of interest were transformed into alanine or they were fully removed from the system both in solvent and in different membrane bilayers. FEP/TI simulations were performed for different peptide/membrane systems using both atomistic and CG force fields, and the results agreed with the experimental findings.

An important aspect of the alchemical free energy calculations on membrane proteins concerns the comparison between the predicted free energy values and those obtained from experimental assays. Surface plasmon resonance (SPR) is one of the most frequently used experimental assays for computing protein/membrane-binding free energies.[190] A typical SPR protocol allows for the measurement of the direct binding of the ligand on a soluble protein. However, the measurement of the binding free energies of ligands to membrane proteins remains a challenging task as the proteins needs to be in their original membranes or deposited in a suitable lipid bilayer or solubilized in a suitable detergents that retain the native structure, conformation and activity of the protein.[191] Recent developments in SPR instrumentation using for instance covalently immobilized antibodies[192] show high potential of the technique to screen for ligand binding to membrane proteins. For this reason, SPR assays have been used for a range of membrane proteins.[193−196] Other techniques such as competitive fluorescence resonance energy transfer (FRET) and isothermal titration calorimetry (ITC) can also measure binding free energies of ligands on membrane proteins.[197,198] Saturation transfer difference (STD) nuclear magnetic resonance (NMR) experiments have been used to measure the unfolding temperature of the β2-adrenergic receptor in a lipidic cubic phase (LCP[199]), which is composed of membrane-like lipid bilayers at high density for studying effects of lipids on membrane protein structure, function and stability as a function of cholesterol concentration.[200] The STD amplification factor values are directly proportional to the cholesterol bound fraction, and they can be used to estimate dissociation constants from the effects on the folding temperature of the receptor at a given cholesterol concentration. Finally, over the past decade, mass spectrometry has also emerged as a powerful technique for quantifying lipid−protein interactions.[201,202]

Despite the recent advances in different experimental assays, one should bear in mind that all of the available methods can introduce significant uncertainties in the measured binding affinities. These errors may arise from the experimental setup (i.e., incorrect local lipid concentration and/or incorrect estimations of binding site occupancy from structural changes or functional response). Alchemical simulations, on the other hand, can also introduce errors on the estimated binding free energies due to force-field limitations or insufficient sampling. However, the main source of uncertainty may arise from ambiguities in the concentration scale and the definition of the standard state when simulating lipid bilayer systems. The latter could also affect the relation of the experimental observables to the binding affinities obtained from FEP/TI calculations. To this end, the SAFEP protocol[59] was employed to tackle this issue by introducing the nonideality of cholesterol:POPC membranes as mentioned in the theoretical framework section. Finally, good consistency with experimental values have been also observed for FEP calculations on three different peripheral membrane proteins.[174]

Alchemical binding free energy predictions are now an integral part of the lead optimization process. The calculations can be difficult to setup and can be sensitive to choices in input preparation, but well-validated RBFE calculations can be performed consistently and with errors approaching 1 kcal/mol. It has been shown that repetitive use of a predictive model with such accuracy can lead to very positive outcomes over the course of a drug discovery program.[203,204] Indeed, FEP methods can be used iteratively as part of recurring design−make−test cycles, leading to increasingly better compounds in less time.[10] As force fields improve, sampling is extended, and we improve and standardize the approaches for system input generation, we may see alchemical RBFE calculations approach the accuracy of the experiment. That poses the question of whether we invest sufficient resources and effort into validating and running our computational assays compared to *in vitro* assays in drug discovery.[205] Turning to the specific case of membrane proteins, we have seen in the examples provided that it is possible to reach similar levels of performance as seen for soluble proteins, and this has impacted not only drug affinity prediction but also understanding of the mechanism of action and protein stability among other aspects. The main caveat is the additional challenge to reach high-quality protein−ligand structures. The best available experimental structures for GPCRs such as A_{2A} have led to multiple successful reports of alchemical methods discussed above, hence the methods are more than feasible. Nevertheless, it is still far more challenging and expensive to reach high-resolution experimental membrane protein structures, although there are specialist approaches and structures are solved by groups in industrial drug discovery.[206−208] It is more likely that membrane protein targets may require the use of model structures. In that case, we described how good results have been reported in the literature, but substantial extra care and thought are needed to validate the input and overall approach.

Finally, we summarize and highlight the most important lessons that emerge from this review. First, alchemical free energy calculations on membrane-associated proteins were shown to produce binding affinity predictions within 1 kcal/mol from experiments for pharmacologically relevant systems including GPCRs and ion channels.[63,116−118,138,141,142,144,145,179,185] Despite their computational burden, these calculations provide significantly more accurate results than QSAR, docking, or end-points approaches and should be integrated in the drug discovery pipeline for lead-optimization and fragment-based screening. In addition, the reached level of accuracy in combination with some macroscopic model[132] opens the way to more ambitious prospective analyses such as the rational design of agonists and antagonists[142] or the predictions of IC50 values[135] with direct pharmacological implications. Second, the accuracy of rigorous binding free energy predictions strongly depends on the quality of the three-dimensional structure of the protein as well as adequate modeling of the physiological environment including the membrane composition, ions, water networks, and the protonation states of ligands. While the former is being

https://doi.org/10.1021/acs.jctc.3c00365
J. Chem. Theory Comput. 2023, 19, 7437−7458

facilitated by the disruptive advent of high-resolution cryo-EM, particularly for membrane-associated proteins,[209] the latter still requires particular care from the free energy practitioner including special treatments and retrospective validations of the ultimate molecular model. In addition, force-field reparameterizations to account for incorrect torsional profiles[117] and/or nonclassical interactions (e.g., halogen bonding, cation−π interactions, etc.) may be critical to obtain accurate predictions. Third, rigorous free energy calculations provide a more detailed understanding of the ligand-binding affinity, which is critical for rational molecular design. For illustration, the separation of the ligand-binding affinity for one GPCR into membrane and site affinity contributions showed that active compounds with improved ADME properties (i.e., less lipophilic) can be designed by optimizing the affinity for the protein.[118] Fourth, the combination of accurate alchemical free energy calculations with end-point approaches[144] or machine-learning methods[24,25] may reduce the computational burden while preserving accuracy. The latter opens up FEP-based high-throughput screening workflows that are expected to flourish in the near future. Last, alchemical free energy calculations provide a service to structural biology beyond binding affinity predictions, e.g., for allosteric binding site search, tautomeric form or protonation state of ligands in the bound state, etc. Overall, we believe that alchemical free energy calculations will be widely used in prospective drug discovery in the coming years, and coupled with the important role that membrane proteins play in disease and drug discovery, we may see an even more important role of these methodologies applied to lead optimization for these important protein families.

AUTHOR INFORMATION

Corresponding Authors

Francesca Deflorian − *Sosei Heptares, Cambridge CB21 6DG, United Kingdom*; Email: Francesca.Deflorian@soseiheptares.com

Gary Tresadern − *CADD, In Silico Discovery, Janssen Research & Development, 2340 Beerse, Belgium*; orcid.org/0000-0002-4801-1644; Email: gtresade@its.jnj.com

Marco Cecchini − *Institut de Chimie de Strasbourg, UMR7177, CNRS, Université de Strasbourg, F-67083 Strasbourg Cedex, France*; orcid.org/0000-0003-2671-1583; Email: mcecchini@unistra.fr

Zoe Cournia − *Biomedical Research Foundation, Academy of Athens, 11527 Athens, Greece*; orcid.org/0000-0001-9287-364X; Email: zcournia@bioacademy.gr

Authors

Michail Papadourakis − *Biomedical Research Foundation, Academy of Athens, 11527 Athens, Greece*; orcid.org/0000-0002-9969-5871

Hryhory Sinenka − *Institut de Chimie de Strasbourg, UMR7177, CNRS, Université de Strasbourg, F-67083 Strasbourg Cedex, France*; orcid.org/0000-0003-3495-7786

Pierre Matricon − *Sosei Heptares, Cambridge CB21 6DG, United Kingdom*

Jérôme Hénin − *Laboratoire de Biochimie Théorique UPR 9080, CNRS and Université Paris Cité, 75005 Paris, France*; orcid.org/0000-0003-2540-4098

Grace Brannigan − *Center for Computational and Integrative Biology, Rutgers University−Camden, Camden, New Jersey 08103, United States of America; Department of Physics, Rutgers University−Camden, Camden, New Jersey 08102, United States of America*; orcid.org/0000-0001-8949-2694

Laura Pérez-Benito − *CADD, In Silico Discovery, Janssen Research & Development, 2340 Beerse, Belgium*

Vineet Pande − *CADD, In Silico Discovery, Janssen Research & Development, 2340 Beerse, Belgium*

Herman van Vlijmen − *CADD, In Silico Discovery, Janssen Research & Development, 2340 Beerse, Belgium*; orcid.org/0000-0002-1915-3141

Chris de Graaf − *Sosei Heptares, Cambridge CB21 6DG, United Kingdom*; orcid.org/0000-0002-1226-2150

Complete contact information is available at: https://pubs.acs.org/10.1021/acs.jctc.3c00365

Author Contributions

The paper was written through contributions of all authors. All authors have given approval to the final version of the paper.

Funding

H.S., M.C., C.d.G., V.P., H.v.V., and Z.C. have been supported by the European Union's Horizon 2020 MSCA Program under grant agreement 956314 (ALLODD). M.P. has been supported by the Bodossaki Foundation Scholarships. J.H. has been supported by Agence Nationale de la Recherche under grant ANR-11-LABX-0011.

Notes

The authors declare no competing financial interest.

ACKNOWLEDGMENTS

The authors thank Ezry Santiago-McRae for providing the graphics for Figure 5.

ABBREVIATIONS

7TM, seven-transmembrane; β_2-AR, β_2 adrenergic receptor; A_1AR, A_1 adenosine receptor; A_{2A}AR, A_{2A} adenosine receptor; A_3AR, A_3 adenosine receptor; AA, all-atom; ABFE, absolute binding free energy; ABFE/REMD, absolute binding free energy calculations with replica exchange molecular dynamics; ADME, absorption, distribution, metabolism, and excretion; cav-1, Caveolin-1; GBSW, generalized Born with a simple switching function; GCS, Gouy−Chapman−Stern; CG, coarse-grained; CIII, *S. cerevisiae* supercomplex structure containing Complex III; CIV, *S. cerevisiae* supercomplex structure containing Complex IV; CL, cardiolipin; cryo-EM, cryogenic electron microscopy; DA, dopamine; DBC, distance-to-bound configuration; DFT, density functional theory; DMPC, dimyristoylphospatidylcholine; DPPC, dipalmitoyl-phospatidylcholine; EEA1, Early Endosome Antigen 1; ELIC, Erwinia ligand-gated ion channel; ESMACS, enhanced sampling of molecular dynamics with approximation of continuum solvent; FBDD, fragment-based drug design; FEP, free energy perturbation; FRET, fluorescence resonance energy transfer; GCMC, Grand Canonical Monte Carlo; GPCRs, G-protein-coupled receptors; hBD-3, human β defensin type 3; hDAT, human DA transporter; hKir6.2, human inward rectifying potassium 6.2; ITC, isothermal titration calorimetry; KIBRA, kidney/brain protein; LCP, lipidic cubic phase; LGICs, ligand-gated ion channels; Lo, liquid-ordered; Ld, liquid-disordered; MAE, mean absolute error; MD, molecular

https://doi.org/10.1021/acs.jctc.3c00365
J. Chem. Theory Comput. 2023, 19, 7437−7458

dynamics; MjNhaP1, Nhap1 of *Methanocaldococcus jannaschii*; MLCL, myocardiolipin; MM/GBSA, molecular mechanics with generalized Born and surface area solvation; MUE, mean unsigned error; MWC, Monod−Wyman−Changeux; NMR, nuclear magnetic resonance; OmpLA, outer membrane phospholipase A; OX2, orexin receptor 2; PC, phosphatidylcholine; PC2, polycystin-2; PI3KC2α, phosphatidylinositol 4-phosphate 3-kinase C2 domain-containing subunit α; PIP, phosphatidylinositol; PIP2, phosphatidylinositol 4,5-bisphosphate; PIP3, phosphatidylinositol 3,4,5-triphosphate; PI-PLC, phosphatidylinositol-specific phospholipase C; PME, particle-mesh Ewald; PMF, potential of mean force; PMPs, peripheral membrane proteins; POPC, palmitoyloleoylphospatidylcholine; POPE, palmitoyloleoylphospatidylethanolamine; POPG, palmitoyloleoylphospatidylglycerol; PS, phosphatidylserine; PT1, prothrombin fragment 1; PTEN, phosphatase and tensin homologue; PTMs, post-translational modifications; RBFE, relative binding free energy; RMSD, root-mean-squared deviation; RMSE, root-mean-square error; RTKs, receptor tyrosine kinases; SAFEP, streamlined alchemical free energy perturbation; SAR, structure−activity relationship; SBDD, structure-based drug discovery; SERT, serotonin transporter; SHIP2, SH2-containing 5′-inositol phosphatase 2; Smurf2, SMAD-specific E3 ubiquitin-protein ligase 2; SPR, surface plasmon resonance; STD, saturation transfer difference; TI, thermodynamic integration; TIES, thermodynamic integration with enhanced sampling; TREK1, TWIK related K+ channel 1; TRPV5, transient receptor potential vanilloid 5

REFERENCES

(1) Cournia, Z.; Chipot, C.; Roux, B.; York, D. M.; Sherman, W. Free Energy Methods in Drug Discovery—Introduction. In *Free Energy Methods in Drug Discovery: Current State and Future Directions*; ACS Symposium Series; American Chemical Society, 2021; Vol. *1397*, pp 1−38. DOI: 10.1021/bk-2021-1397.ch001.

(2) Armacost, K. A.; Riniker, S.; Cournia, Z. Novel Directions in Free Energy Methods and Applications. *J. Chem. Inf. Model.* **2020**, *60* (1), 1−5.

(3) Chipot, C. Frontiers in Free-Energy Calculations of Biological Systems. *WIREs Computational Molecular Science* **2014**, *4* (1), 71−89.

(4) Mey, A. S. J. S.; Allen, B. K.; Bruce Macdonald, H. E.; Chodera, J. D.; Hahn, D. F.; Kuhn, M.; Michel, J.; Mobley, D. L.; Naden, L. N.; Prasad, S.; Rizzi, A.; Scheen, J.; Shirts, M. R.; Tresadern, G.; Xu, H. Best Practices for Alchemical Free Energy Calculations [Article v1.0]. *Living J. Comput. Mol. Sci.* **2020**, *2* (1), 18378.

(5) Cournia, Z.; Allen, B.; Sherman, W. Relative Binding Free Energy Calculations in Drug Discovery: Recent Advances and Practical Considerations. *J. Chem. Inf. Model.* **2017**, *57* (12), 2911−2937.

(6) Aldeghi, M.; Heifetz, A.; Bodkin, M. J.; Knapp, S.; Biggin, P. C. Accurate Calculation of the Absolute Free Energy of Binding for Drug Molecules. *Chem. Sci.* **2016**, *7* (1), 207−218.

(7) Wang, E.; Sun, H.; Wang, J.; Wang, Z.; Liu, H.; Zhang, J. Z. H.; Hou, T. End-Point Binding Free Energy Calculation with MM/PBSA and MM/GBSA: Strategies and Applications in Drug Design. *Chem. Rev.* **2019**, *119* (16), 9478−9508.

(8) Torrie, G. M.; Valleau, J. P. Nonphysical Sampling Distributions in Monte Carlo Free-Energy Estimation: Umbrella Sampling. *J. Comput. Phys.* **1977**, *23* (2), 187−199.

(9) (a) Laio, A.; Parrinello, M. Escaping free-energy minima. *Proceedings of the National Academy of Sciences* **2002**, *99* (20), 12562−12566. (b) Bussi, G.; Branduardi, D. Free-energy calculations with metadynamics: theory and practice. *Reviews in Computational Chemistry* **2015**, *28*, 1−49.

(10) Tresadern, G.; Velter, I.; Trabanco, A. A.; Van den Keybus, F.; Macdonald, G. J.; Somers, M. V. F.; Vanhoof, G.; Leonard, P. M.; Lamers, M. B. A. C.; Van Roosbroeck, Y. E. M.; Buijnsters, P. J. J. A. [1,2,4]Triazolo[1,5-a]Pyrimidine Phosphodiesterase 2A Inhibitors: Structure and Free-Energy Perturbation-Guided Exploration. *J. Med. Chem.* **2020**, *63* (21), 12887−12910.

(11) Majellaro, M.; Jespers, W.; Crespo, A.; Núñez, M. J.; Novio, S.; Azuaje, J.; Prieto-Díaz, R.; Gioé, C.; Alispahic, B.; Brea, J.; Loza, M. I.; Freire-Garabal, M.; Garcia-Santiago, C.; Rodríguez-García, C.; García-Mera, X.; Caamaño, O.; Fernandez-Masaguer, C.; Sardina, J. F.; Stefanachi, A.; El Maatougui, A.; Mallo-Abreu, A.; Åqvist, J.; Gutiérrez-de-Terán, H.; Sotelo, E. 3,4-Dihydropyrimidin-2(1H)-Ones as Antagonists of the Human A2B Adenosine Receptor: Optimization, Structure−Activity Relationship Studies, and Enantiospecific Recognition. *J. Med. Chem.* **2021**, *64* (1), 458−480.

(12) Wang, L.; Wu, Y.; Deng, Y.; Kim, B.; Pierce, L.; Krilov, G.; Lupyan, D.; Robinson, S.; Dahlgren, M. K.; Greenwood, J.; Romero, D. L.; Masse, C.; Knight, J. L.; Steinbrecher, T.; Beuming, T.; Damm, W.; Harder, E.; Sherman, W.; Brewer, M.; Wester, R.; Murcko, M.; Frye, L.; Farid, R.; Lin, T.; Mobley, D. L.; Jorgensen, W. L.; Berne, B. J.; Friesner, R. A.; Abel, R. Accurate and Reliable Prediction of Relative Ligand Binding Potency in Prospective Drug Discovery by Way of a Modern Free-Energy Calculation Protocol and Force Field. *J. Am. Chem. Soc.* **2015**, *137* (7), 2695−2703.

(13) Mendoza-Martinez, C.; Papadourakis, M.; Llabres, S.; Gupta, A. A.; Barlow, P. N.; Michel, J. Energetics of a Protein Disorder−Order Transition in Small Molecule Recognition. *Chemical Science* **2022**, *13* (18), 5220−5229.

(14) Mortier, J.; Friberg, A.; Badock, V.; Moosmayer, D.; Schroeder, J.; Steigemann, P.; Siegel, F.; Gradl, S.; Bauser, M.; Hillig, R. C.; Briem, H.; Eis, K.; Bader, B.; Nguyen, D.; Christ, C. D. Computationally Empowered Workflow Identifies Novel Covalent Allosteric Binders for KRASG12C. *ChemMedChem.* **2020**, *15* (10), 827−832.

(15) O' Donovan, D. H.; Gregson, C.; Packer, M. J.; Greenwood, R.; Pike, K. G.; Kawatkar, S.; Bloecher, A.; Robinson, J.; Read, J.; Code, E.; Hsu, J. H.-R.; Shen, M.; Woods, H.; Barton, P.; Fillery, S.; Williamson, B.; Rawlins, P. B.; Bagal, S. K. Free Energy Perturbation in the Design of EED Ligands as Inhibitors of Polycomb Repressive Complex 2 (PRC2) Methyltransferase. *Bioorg. Med. Chem. Lett.* **2021**, *39*, No. 127904.

(16) Gapsys, V.; Perez-Benito, L.; Aldeghi, M.; Seeliger, D.; van Vlijmen, H.; Tresadern, G.; de Groot, B. L. Large Scale Relative Protein Ligand Binding Affinities Using Non-Equilibrium Alchemy. *Chem. Sci.* **2020**, *11* (4), 1140−1152.

(17) Schindler, C. E. M.; Baumann, H.; Blum, A.; Böse, D.; Buchstaller, H.-P.; Burgdorf, L.; Cappel, D.; Chekler, E.; Czodrowski, P.; Dorsch, D.; Eguida, M. K. I.; Follows, B.; Fuchß, T.; Grädler, U.; Gunera, J.; Johnson, T.; Jorand Lebrun, C.; Karra, S.; Klein, M.; Knehans, T.; Koetzner, L.; Krier, M.; Leiendecker, M.; Leuthner, B.; Li, L.; Mochalkin, I.; Musil, D.; Neagu, C.; Rippmann, F.; Schiemann, K.; Schulz, R.; Steinbrecher, T.; Tanzer, E.-M.; Unzue Lopez, A.; Viacava Follis, A.; Wegener, A.; Kuhn, D. Large-Scale Assessment of Binding Free Energy Calculations in Active Drug Discovery Projects. *J. Chem. Inf. Model.* **2020**, *60* (11), 5457−5474.

(18) Rizzi, A.; Jensen, T.; Slochower, D. R.; Aldeghi, M.; Gapsys, V.; Ntekoumes, D.; Bosisio, S.; Papadourakis, M.; Henriksen, N. M.; de Groot, B. L.; Cournia, Z.; Dickson, A.; Michel, J.; Gilson, M. K.; Shirts, M. R.; Mobley, D. L.; Chodera, J. D. The SAMPL6 SAMPLing Challenge: Assessing the Reliability and Efficiency of Binding Free Energy Calculations. *J. Comput. Aided Mol. Des* **2020**, *34* (5), 601−633.

(19) Zhang, C.-H.; Stone, E. A.; Deshmukh, M.; Ippolito, J. A.; Ghahremanpour, M. M.; Tirado-Rives, J.; Spasov, K. A.; Zhang, S.; Takeo, Y.; Kudalkar, S. N.; Liang, Z.; Isaacs, F.; Lindenbach, B.; Miller, S. J.; Anderson, K. S.; Jorgensen, W. L. Potent Noncovalent Inhibitors of the Main Protease of SARS-CoV-2 from Molecular Sculpting of the Drug Perampanel Guided by Free Energy Perturbation Calculations. *ACS Cent. Sci.* **2021**, *7* (3), 467−475.

(20) Zavitsanou, S.; Tsengenes, A.; Papadourakis, M.; Amendola, G.; Chatzigoulas, A.; Dellis, D.; Cosconati, S.; Cournia, Z. FEPrepare: A

Web-Based Tool for Automating the Setup of Relative Binding Free Energy Calculations. *J. Chem. Inf. Model.* **2021**, *61* (9), 4131−4138.
(21) Fu, H.; Chen, H.; Cai, W.; Shao, X.; Chipot, C. BFEE2: Automated, Streamlined, and Accurate Absolute Binding Free-Energy Calculations. *J. Chem. Inf. Model.* **2021**, *61* (5), 2116−2123.
(22) Gapsys, V.; Hahn, D. F.; Tresadern, G.; Mobley, D. L.; Rampp, M.; de Groot, B. L. Pre-Exascale Computing of Protein−Ligand Binding Free Energies with Open Source Software for Drug Design. *J. Chem. Inf. Model.* **2022**, *62* (5), 1172−1177.
(23) Chen, W.; Cui, D.; Jerome, S. V.; Michino, M.; Lenselink, E. B.; Huggins, D. J.; Beautrait, A.; Vendome, J.; Abel, R.; Friesner, R. A.; Wang, L. Enhancing Hit Discovery in Virtual Screening through Accurate Calculation of Absolute Protein-Ligand Binding Free Energies. *J. Chem. Inf. Model.* **2023**, *63* (10), 3171−3195.
(24) Konze, K. D.; Bos, P. H.; Dahlgren, M. K.; Leswing, K.; Tubert-Brohman, I.; Bortolato, A.; Robbason, B.; Abel, R.; Bhat, S. Reaction-Based Enumeration, Active Learning, and Free Energy Calculations To Rapidly Explore Synthetically Tractable Chemical Space and Optimize Potency of Cyclin-Dependent Kinase 2 Inhibitors. *J. Chem. Inf. Model.* **2019**, *59* (9), 3782−3793.
(25) Khalak, Y.; Tresadern, G.; Hahn, D. F.; de Groot, B. L.; Gapsys, V. Chemical Space Exploration with Active Learning and Alchemical Free Energies. *J. Chem. Theory Comput.* **2022**, *18* (10), 6259−6270.
(26) Salomon-Ferrer, R.; Götz, A. W.; Poole, D.; Le Grand, S.; Walker, R. C. Routine Microsecond Molecular Dynamics Simulations with AMBER on GPUs. 2. Explicit Solvent Particle Mesh Ewald. *J. Chem. Theory Comput* **2013**, *9* (9), 3878−3888.
(27) Götz, A. W.; Williamson, M. J.; Xu, D.; Poole, D.; Le Grand, S.; Walker, R. C. Routine Microsecond Molecular Dynamics Simulations with AMBER on GPUs. 1. Generalized Born. *J. Chem. Theory Comput.* **2012**, *8* (5), 1542−1555.
(28) Harvey, M. J.; Giupponi, G.; Fabritiis, G. D. ACEMD: Accelerating Biomolecular Dynamics in the Microsecond Time Scale. *J. Chem. Theory Comput.* **2009**, *5* (6), 1632−1639.
(29) Eastman, P.; Friedrichs, M. S.; Chodera, J. D.; Radmer, R. J.; Bruns, C. M.; Ku, J. P.; Beauchamp, K. A.; Lane, T. J.; Wang, L.-P.; Shukla, D.; Tye, T.; Houston, M.; Stich, T.; Klein, C.; Shirts, M. R.; Pande, V. S. OpenMM 4: A Reusable, Extensible, Hardware Independent Library for High Performance Molecular Simulation. *J. Chem. Theory Comput.* **2013**, *9* (1), 461−469.
(30) Bergdorf, M.; Baxter, S.; Rendleman, C. A.; Shaw, D. E. Desmond/GPU Performance as of November 2016.
(31) Kirkwood, J. G. Statistical Mechanics of Fluid Mixtures. *J. Chem. Phys.* **1935**, *3* (5), 300−313.
(32) Zwanzig, R. W. High-Temperature Equation of State by a Perturbation Method. I. Nonpolar Gases. *J. Chem. Phys.* **1954**, *22* (8), 1420−1426.
(33) Pierce, L. C.T.; Salomon-Ferrer, R.; Augusto F. de Oliveira, C.; McCammon, J. A.; Walker, R. C. Routine Access to Millisecond Time Scale Events with Accelerated Molecular Dynamics. *J. Chem. Theory Comput.* **2012**, *8* (9), 2997−3002.
(34) Gapsys, V.; Yildirim, A.; Aldeghi, M.; Khalak, Y.; van der Spoel, D.; de Groot, B. L. Accurate Absolute Free Energies for Ligand−Protein Binding Based on Non-Equilibrium Approaches. *Commun. Chem.* **2021**, *4* (1), 1−13.
(35) Khalak, Y.; Tresadern, G.; Aldeghi, M.; Baumann, H. M.; Mobley, D. L.; de Groot, B. L.; Gapsys, V. Alchemical Absolute Protein−Ligand Binding Free Energies for Drug Design. *Chem. Sci.* **2021**, *12* (41), 13958−13971.
(36) Rombouts, F. J. R.; Tresadern, G.; Buijnsters, P.; Langlois, X.; Tovar, F.; Steinbrecher, T. B.; Vanhoof, G.; Somers, M.; Andrés, J.-I.; Trabanco, A. A. Pyrido[4,3-e][1,2,4]Triazolo[4,3-a]Pyrazines as Selective, Brain Penetrant Phosphodiesterase 2 (PDE2) Inhibitors. *ACS Med. Chem. Lett.* **2015**, *6* (3), 282−286.
(37) Steinbrecher, T.; Zhu, C.; Wang, L.; Abel, R.; Negron, C.; Pearlman, D.; Feyfant, E.; Duan, J.; Sherman, W. Predicting the Effect of Amino Acid Single-Point Mutations on Protein Stability—Large-Scale Validation of MD-Based Relative Free Energy Calculations. *J. Mol. Biol.* **2017**, *429* (7), 948−963.
(38) Clark, A. J.; Gindin, T.; Zhang, B.; Wang, L.; Abel, R.; Murret, C. S.; Xu, F.; Bao, A.; Lu, N. J.; Zhou, T.; Kwong, P. D.; Shapiro, L.; Honig, B.; Friesner, R. A. Free Energy Perturbation Calculation of Relative Binding Free Energy between Broadly Neutralizing Antibodies and the Gp120 Glycoprotein of HIV-1. *J. Mol. Biol.* **2017**, *429* (7), 930−947.
(39) Duboué-Dijon, E.; Hénin, J. Building Intuition for Binding Free Energy Calculations: Bound State Definition, Restraints, and Symmetry. *J. Chem. Phys.* **2021**, *154* (20), No. 204101.
(40) Montalvo-Acosta, J. J.; Cecchini, M. Computational Approaches to the Chemical Equilibrium Constant in Protein-Ligand Binding. *Molecular Informatics* **2016**, *35* (11−12), 555−567.
(41) Cournia, Z.; Allen, T. W.; Andricioaei, I.; Antonny, B.; Baum, D.; Brannigan, G.; Buchete, N.-V.; Deckman, J. T.; Delemotte, L.; del Val, C.; Friedman, R.; Gkeka, P.; Hege, H.-C.; Hénin, J.; Kasimova, M. A.; Kolocouris, A.; Klein, M. L.; Khalid, S.; Lemieux, M. J.; Lindow, N.; Roy, M.; Selent, J.; Tarek, M.; Tofoleanu, F.; Vanni, S.; Urban, S.; Wales, D. J.; Smith, J. C.; Bondar, A.-N. Membrane Protein Structure, Function and Dynamics: A Perspective from Experiments and Theory. *J. Membr. Biol.* **2015**, *248* (4), 611−640.
(42) Chatzigoulas, A.; Cournia, Z. Rational Design of Allosteric Modulators: Challenges and Successes. *WIREs Computational Molecular Science* **2021**, *11* (6), No. e1529.
(43) Hocker, H. J.; Cho, K.-J.; Chen, C.-Y. K.; Rambahal, N.; Sagineedu, S. R.; Shaari, K.; Stanslas, J.; Hancock, J. F.; Gorfe, A. A. Andrographolide Derivatives Inhibit Guanine Nucleotide Exchange and Abrogate Oncogenic Ras Function. *Proc. Natl. Acad. Sci. U. S. A.* **2013**, *110* (25), 10201−10206.
(44) Cerdan, A. H.; Sisquellas, M.; Pereira, G.; Barreto Gomes, D. E.; Changeux, J.-P.; Cecchini, M. The Glycine Receptor Allosteric Ligands Library (GRALL). *Bioinformatics* **2020**, *36* (11), 3379−3384.
(45) Bagal, S. K.; Brown, A. D.; Cox, P. J.; Omoto, K.; Owen, R. M.; Pryde, D. C.; Sidders, B.; Skerratt, S. E.; Stevens, E. B.; Storer, R. I.; Swain, N. A. Ion Channels as Therapeutic Targets: A Drug Discovery Perspective. *J. Med. Chem.* **2013**, *56* (3), 593−624.
(46) Chan, H. C. S.; Li, Y.; Dahoun, T.; Vogel, H.; Yuan, S. New Binding Sites, New Opportunities for GPCR Drug Discovery. *Trends Biochem. Sci.* **2019**, *44* (4), 312−330.
(47) Hénin, J.; Pohorille, A.; Chipot, C. Insights into the Recognition and Association of Transmembrane α-Helices. The Free Energy of α-Helix Dimerization in Glycophorin A. *J. Am. Chem. Soc.* **2005**, *127* (23), 8478−8484.
(48) Hénin, J.; Maigret, B.; Tarek, M.; Escrieut, C.; Fourmy, D.; Chipot, C. Probing a Model of a GPCR/Ligand Complex in an Explicit Membrane Environment: The Human Cholecystokinin-1 Receptor. *Biophys. J.* **2006**, *90* (4), 1232−1240.
(49) Noskov, S. Y. Molecular mechanism of substrate specificity in the bacterial neutral amino acid transporter LeuT. *Proteins: Struct., Funct., Bioinf.* **2008**, *73* (4), 851−863.
(50) Heinzelmann, G.; Baştuğ, T.; Kuyucak, S. Free Energy Simulations of Ligand Binding to the Aspartate Transporter GltPh. *Biophys. J.* **2011**, *101* (10), 2380−2388.
(51) Lenselink, E. B.; Louvel, J.; Forti, A. F.; van Veldhoven, J. P. D.; de Vries, H.; Mulder-Krieger, T.; McRobb, F. M.; Negri, A.; Goose, J.; Abel, R.; van Vlijmen, H. W. T.; Wang, L.; Harder, E.; Sherman, W.; IJzerman, A. P.; Beuming, T. Predicting Binding Affinities for GPCR Ligands Using Free-Energy Perturbation. *ACS Omega* **2016**, *1* (2), 293−304.
(52) Deflorian, F.; Perez-Benito, L.; Lenselink, E. B.; Congreve, M.; van Vlijmen, H. W. T.; Mason, J. S.; Graaf, C. de; Tresadern, G. Accurate Prediction of GPCR Ligand Binding Affinity with Free Energy Perturbation. *J. Chem. Inf. Model.* **2020**, *60* (11), 5563−5579.
(53) Jespers, W.; Heitman, L. H.; IJzerman, A. P.; Sotelo, E.; van Westen, G. J. P.; Åqvist, J.; Gutiérrez-de-Terán, H. Deciphering Conformational Selectivity in the A2A Adenosine G Protein-Coupled Receptor by Free Energy Simulations. *PLOS Computational Biology* **2021**, *17* (11), No. e1009152.

https://doi.org/10.1021/acs.jctc.3c00365
J. Chem. Theory Comput. 2023, 19, 7437−7458

(54) Oakes, V.; Domene, C. Capturing the Molecular Mechanism of Anesthetic Action by Simulation Methods. *Chem. Rev.* **2019**, *119* (9), 5998−6014.
(55) Crnjar, A.; Comitani, F.; Melis, C.; Molteni, C. Mutagenesis Computer Experiments in Pentameric Ligand-Gated Ion Channels: The Role of Simulation Tools with Different Resolution. *Interface Focus* **2019**, *9* (3), No. 20180067.
(56) Flood, E.; Boiteux, C.; Lev, B.; Vorobyov, I.; Allen, T. W. Atomistic Simulations of Membrane Ion Channel Conduction, Gating, and Modulation. *Chem. Rev.* **2019**, *119* (13), 7737−7832.
(57) Şterbuleac, D. Molecular Dynamics: A Powerful Tool for Studying the Medicinal Chemistry of Ion Channel Modulators. *RSC Med. Chem.* **2021**, *12* (9), 1503−1518.
(58) Bignucolo, O.; Chipot, C.; Kellenberger, S.; Roux, B. Galvani Offset Potential and Constant-PH Simulations of Membrane Proteins. *J. Phys. Chem. B* **2022**, *126* (36), 6868−6877.
(59) Salari, R.; Joseph, T.; Lohia, R.; Hénin, J.; Brannigan, G. A Streamlined, General Approach for Computing Ligand Binding Free Energies and Its Application to GPCR-Bound Cholesterol. *J. Chem. Theory Comput.* **2018**, *14* (12), 6560−6573.
(60) Clark, F.; Robb, G.; Cole, D. J.; Michel, J. Comparison of Receptor-Ligand Restraint Schemes for Alchemical Absolute Binding Free Energy Calculations. *J. Chem. Theory Comput.* **2023**, *19*, 3686−3704.
(61) Boresch, S.; Tettinger, F.; Leitgeb, M.; Karplus, M. Absolute Binding Free Energies: A Quantitative Approach for Their Calculation. *J. Phys. Chem. B* **2003**, *107* (35), 9535−9551.
(62) Zhao, C.; Caplan, D. A.; Noskov, S. Yu. Evaluations of the Absolute and Relative Free Energies for Antidepressant Binding to the Amino Acid Membrane Transporter LeuT with Free Energy Simulations. *J. Chem. Theory Comput.* **2010**, *6* (6), 1900−1914.
(63) Lai, P.-K.; Kaznessis, Y. N. Free Energy Calculations of Microcin J25 Variants Binding to the FhuA Receptor. *J. Chem. Theory Comput.* **2017**, *13* (7), 3413−3423.
(64) Ebrahimi, M.; Hénin, J. Symmetry-Adapted Restraints for Binding Free Energy Calculations. *J. Chem. Theory Comput.* **2022**, *18* (4), 2494−2502.
(65) Corey, R. A.; Vickery, O. N.; Sansom, M. S. P.; Stansfeld, P. J. Insights into Membrane Protein−Lipid Interactions from Free Energy Calculations. *J. Chem. Theory Comput.* **2019**, *15* (10), 5727−5736.
(66) Jiang, W.; Lacroix, J.; Luo, Y. L. Importance of Molecular Dynamics Equilibrium Protocol on Protein-Lipid Interaction near Channel Pore. *Biophysical Reports* **2022**, *2* (4), No. 100080.
(67) Petroff, J. T.; Dietzen, N. M.; Santiago-McRae, E.; Deng, B.; Washington, M. S.; Chen, L. J.; Trent Moreland, K.; Deng, Z.; Rau, M.; Fitzpatrick, J. A. J.; Yuan, P.; Joseph, T. T.; Hénin, J.; Brannigan, G.; Cheng, W. W. L. Open-Channel Structure of a Pentameric Ligand-Gated Ion Channel Reveals a Mechanism of Leaflet-Specific Phospholipid Modulation. *Nat. Commun.* **2022**, *13* (1), 7017.
(68) Joseph, T. T.; Bu, W.; Lin, W.; Zoubak, L.; Yeliseev, A.; Liu, R.; Eckenhoff, R. G.; Brannigan, G. Ketamine Metabolite (2R,6R)-Hydroxynorketamine Interacts with μ and κ Opioid Receptors. *ACS Chem. Neurosci.* **2021**, *12* (9), 1487−1497.
(69) Kjølbye, L. R.; Pereira, G. P.; Bartocci, A.; Pannuzzo, M.; Albani, S.; Marchetto, A.; Jiménez-García, B.; Martin, J.; Rossetti, G.; Cecchini, M.; Wu, S.; Monticelli, L.; Souza, P. C. T. Towards Design of Drugs and Delivery Systems with the Martini Coarse-Grained Model. *QRB Discovery* **2022**, *3*, e19.
(70) Darden, T.; York, D.; Pedersen, L. Particle Mesh Ewald: An N·log(N) Method for Ewald Sums in Large Systems. *J. Chem. Phys.* **1993**, *98* (12), 10089−10092.
(71) Lin, Y.-L.; Aleksandrov, A.; Simonson, T.; Roux, B. An Overview of Electrostatic Free Energy Computations for Solutions and Proteins. *J. Chem. Theory Comput.* **2014**, *10* (7), 2690−2709.
(72) Hummer, G.; Pratt, L. R.; García, A. E. Free Energy of Ionic Hydration. *J. Phys. Chem.* **1996**, *100* (4), 1206−1215.
(73) Rashid, M. H.; Heinzelmann, G.; Huq, R.; Tajhya, R. B.; Chang, S. C.; Chhabra, S.; Pennington, M. W.; Beeton, C.; Norton, R. S.; Kuyucak, S. A Potent and Selective Peptide Blocker of the Kv1.3 Channel: Prediction from Free-Energy Simulations and Experimental Confirmation. *PLoS One* **2013**, *8* (11), No. e78712.
(74) Heinzelmann, G.; Chen, P.-C.; Kuyucak, S. Computation of Standard Binding Free Energies of Polar and Charged Ligands to the Glutamate Receptor GluA2. *J. Phys. Chem. B* **2014**, *118* (7), 1813−1824.
(75) Simonson, T.; Roux, B. Concepts and Protocols for Electrostatic Free Energies. *Mol. Simul.* **2016**, *42* (13), 1090−1101.
(76) Wu, Z.; Biggin, P. C. Correction Schemes for Absolute Binding Free Energies Involving Lipid Bilayers. *J. Chem. Theory Comput.* **2022**, *18* (4), 2657−2672.
(77) Rocklin, G. J.; Mobley, D. L.; Dill, K. A.; Hünenberger, P. H. Calculating the Binding Free Energies of Charged Species Based on Explicit-Solvent Simulations Employing Lattice-Sum Methods: An Accurate Correction Scheme for Electrostatic Finite-Size Effects. *J. Chem. Phys.* **2013**, *139* (18), No. 184103.
(78) Hahn, D. F.; Bayly, C. I.; Boby, M. L; Bruce Macdonald, H. E.; Chodera, J. D.; Gapsys, V.; Mey, A. S. J. S.; Mobley, D. L.; Benito, L. P.; Schindler, C. E. M.; Tresadern, G.; Warren, G. L. Best Practices for Constructing, Preparing, and Evaluating Protein-Ligand Binding Affinity Benchmarks [Article v1.0]. *Living Journal of Computational Molecular Science* **2022**, *4* (1), 1497−1497.
(79) Venkatakrishnan, A. J.; Deupi, X.; Lebon, G.; Heydenreich, F. M.; Flock, T.; Miljus, T.; Balaji, S.; Bouvier, M.; Veprintsev, D. B.; Tate, C. G.; Schertler, G. F. X.; Babu, M. M. Diverse Activation Pathways in Class A GPCRs Converge near the G-Protein-Coupling Region. *Nature* **2016**, *536* (7617), 484−487.
(80) Mason, J. S.; Bortolato, A.; Weiss, D. R.; Deflorian, F.; Tehan, B.; Marshall, F. H. High End GPCR Design: Crafted Ligand Design and Druggability Analysis Using Protein Structure, Lipophilic Hotspots and Explicit Water Networks. *In Silico Pharmacol.* **2013**, *1* (1), 23.
(81) Zhou, Q.; Yang, D.; Wu, M.; Guo, Y.; Guo, W.; Zhong, L.; Cai, X.; Dai, A.; Jang, W.; Shakhnovich, E. I.; Liu, Z.-J.; Stevens, R. C.; Lambert, N. A.; Babu, M. M.; Wang, M.-W.; Zhao, S. Common Activation Mechanism of Class A GPCRs. *eLife* **2019**, *8*, No. e50279.
(82) Venkatakrishnan, A. J.; Ma, A. K.; Fonseca, R.; Latorraca, N. R.; Kelly, B.; Betz, R. M.; Asawa, C.; Kobilka, B. K.; Dror, R. O. Diverse GPCRs Exhibit Conserved Water Networks for Stabilization and Activation. *Proc. Natl. Acad. Sci. U. S. A.* **2019**, *116* (8), 3288−3293.
(83) Abel, R.; Young, T.; Farid, R.; Berne, B. J.; Friesner, R. A. Role of the Active-Site Solvent in the Thermodynamics of Factor Xa Ligand Binding. *J. Am. Chem. Soc.* **2008**, *130* (9), 2817−2831.
(84) Truchon, J.-F.; Pettitt, B. M.; Labute, P. A Cavity Corrected 3D-RISM Functional for Accurate Solvation Free Energies. *J. Chem. Theory Comput.* **2014**, *10* (3), 934−941.
(85) Nguyen, C. N.; Kurtzman Young, T.; Gilson, M. K. Grid Inhomogeneous Solvation Theory: Hydration Structure and Thermodynamics of the Miniature Receptor Cucurbit[7]Uril. *J. Chem. Phys.* **2012**, *137* (4), No. 044101.
(86) Braun, E.; Gilmer, J.; Mayes, H. B.; Mobley, D. L.; Monroe, J. I.; Prasad, S.; Zuckerman, D. M. Best Practices for Foundations in Molecular Simulations [Article v1.0]. *Living J. Comput. Mol. Sci.* **2019**, *1* (1), 5957.
(87) Adams, D. J. Chemical Potential of Hard-Sphere Fluids by Monte Carlo Methods. *Mol. Phys.* **1974**, *28* (5), 1241−1252.
(88) Marrone, T. J.; McCammon, J. A.; Resat, H.; Hodge, C. N.; Chang, C.-H. Solvation Studies of DMP323 and A76928 Bound to HIV Protease: Analysis of Water Sites Using Grand Canonical Monte Carlo Simulations. *Protein Sci.* **1998**, *7* (3), 573−579.
(89) Ross, G. A.; Bodnarchuk, M. S.; Essex, J. W. Water Sites, Networks, And Free Energies with Grand Canonical Monte Carlo. *J. Am. Chem. Soc.* **2015**, *137* (47), 14930−14943.
(90) Preininger, A. M.; Meiler, J.; Hamm, H. Conformational Flexibility and Structural Dynamics in GPCR-Mediated G Protein Activation: A Perspective. *J. Mol. Biol.* **2013**, *425* (13), 2288−2298.
(91) Katritch, V.; Fenalti, G.; Abola, E. E.; Roth, B. L.; Cherezov, V.; Stevens, R. C. Allosteric Sodium in Class A GPCR Signaling. *Trends Biochem. Sci.* **2014**, *39* (5), 233−244.

https://doi.org/10.1021/acs.jctc.3c00365
J. Chem. Theory Comput. 2023, 19, 7437−7458

(92) Liu, W.; Chun, E.; Thompson, A. A.; Chubukov, P.; Xu, F.; Katritch, V.; Han, G. W.; Roth, C. B.; Heitman, L. H.; IJzerman, A. P.; Cherezov, V.; Stevens, R. C. Structural Basis for Allosteric Regulation of GPCRs by Sodium Ions. *Science* **2012**, *337* (6091), 232−236.
(93) Park, S.; Choi, Y. K.; Kim, S.; Lee, J.; Im, W. CHARMM-GUI Membrane Builder for Lipid Nanoparticles with Ionizable Cationic Lipids and PEGylated Lipids. *J. Chem. Inf. Model.* **2021**, *61* (10), 5192−5202.
(94) Humphrey, W.; Dalke, A.; Schulten, K. VMD: Visual Molecular Dynamics. *J. Mol. Graphics* **1996**, *14* (1), 33−38.
(95) Schott-Verdugo, S.; Gohlke, H. PACKMOL-Memgen: A Simple-To-Use, Generalized Workflow for Membrane-Protein−Lipid-Bilayer System Building. *J. Chem. Inf. Model.* **2019**, *59* (6), 2522−2528.
(96) *Schrödinger Release 2023-1: Maestro*; Schrödinger, LLC: New York, NY, 2023.
(97) Case, D. A.; Aktulga, H. M.; Belfon, K.; Ben-Shalom, I. Y., Berryman, J. T.; Brozell, S. R.; Cerutti, D. S.; Cheatham, T. E., III; Cisneros, G. A.; Cruzeiro, V. W. D.; Darden, T. A.; Duke, R. E.; Giambasu, G.; Gilson, M. K.; Gohlke, H.; Goetz, A. W.; Harris, R.; Izadi, S.; Izmailov, S. A.; Kasavajhala, K.; Kaymak, M. C.; King, E.; Kovalenko, A.; Kurtzman, T.; Lee, T. S.; LeGrand, S.; Li, P.; Lin, C.; Liu, J.; Luchko, T.; Luo, R.; Machado, M.; Man, V.; Manathunga, M.; Merz, K. M.; Miao, Y.; Mikhailovskii, O.; Monard, G.; Nguyen, H.; O'Hearn, K. A., Onufriev, A.; Pan, F.; Pantano, S.; Qi, R.; Rahnamoun, A.; Roe, D. R.; Roitberg, A.; Sagui, C.; Schott-Verdugo, S., Shajan, A.; Shen, J.; Simmerling, C. L.; Skrynnikov, N. R.; Smith, J.; Swails, J.; Walker, R. C.; Wang, J.; Wang, J.; Wei, H.; Wolf, R. M.; Wu, X.; Xiong, Y.; Xue, Y.; York, D. M.; Zhao, S.; Kollman, P.A. *Amber 2022*; University of California, San Francisco: San Francisco, 2022.
(98) Dickson, C. J.; Walker, R. C.; Gould, I. R. Lipid21: Complex Lipid Membrane Simulations with AMBER. *J. Chem. Theory Comput.* **2022**, *18* (3), 1726−1736.
(99) Reif, M. M.; Winger, M.; Oostenbrink, C. Testing of the GROMOS Force-Field Parameter Set 54A8: Structural Properties of Electrolyte Solutions, Lipid Bilayers, and Proteins. *J. Chem. Theory Comput.* **2013**, *9* (2), 1247−1264.
(100) Ermilova, I.; Lyubartsev, A. P. Extension of the Slipids Force Field to Polyunsaturated Lipids. *J. Phys. Chem. B* **2016**, *120* (50), 12826−12842.
(101) Huang, J.; MacKerell, A. D. CHARMM36 All-Atom Additive Protein Force Field: Validation Based on Comparison to NMR Data. *J. Comput. Chem.* **2013**, *34* (25), 2135−2145.
(102) Cordomí, A.; Caltabiano, G.; Pardo, L. Membrane Protein Simulations Using AMBER Force Field and Berger Lipid Parameters. *J. Chem. Theory Comput.* **2012**, *8* (3), 948−958.
(103) Abraham, M. J.; Murtola, T.; Schulz, R.; Páll, S.; Smith, J. C.; Hess, B.; Lindahl, E. GROMACS: High Performance Molecular Simulations through Multi-Level Parallelism from Laptops to Supercomputers. *SoftwareX* **2015**, *1−2*, 19−25.
(104) Qiu, Y.; Smith, D. G. A.; Boothroyd, S.; Jang, H.; Hahn, D. F.; Wagner, J.; Bannan, C. C.; Gokey, T.; Lim, V. T.; Stern, C. D.; Rizzi, A.; Tjanaka, B.; Tresadern, G.; Lucas, X.; Shirts, M. R.; Gilson, M. K.; Chodera, J. D.; Bayly, C. I.; Mobley, D. L.; Wang, L.-P. Development and Benchmarking of Open Force Field v1.0.0—the Parsley Small-Molecule Force Field. *J. Chem. Theory Comput.* **2021**, *17* (10), 6262−6280.
(105) Pluhackova, K.; Kirsch, S. A.; Han, J.; Sun, L.; Jiang, Z.; Unruh, T.; Böckmann, R. A. A Critical Comparison of Biomembrane Force Fields: Structure and Dynamics of Model DMPC, POPC, and POPE Bilayers. *J. Phys. Chem. B* **2016**, *120* (16), 3888−3903.
(106) Bacle, A.; Buslaev, P.; Garcia-Fandino, R.; Favela-Rosales, F.; Mendes Ferreira, T.; Fuchs, P. F. J.; Gushchin, I.; Javanainen, M.; Kiirikki, A. M.; Madsen, J. J.; Melcr, J.; Milán Rodríguez, P.; Miettinen, M. S.; Ollila, O. H. S.; Papadopoulos, C. G.; Peón, A.; Piggot, T. J.; Piñeiro, Á.; Virtanen, S. I. Inverse Conformational Selection in Lipid−Protein Binding. *J. Am. Chem. Soc.* **2021**, *143* (34), 13701−13709.
(107) Xu, B.; Vasile, S.; Østergaard, S.; Paulsson, J. F.; Pruner, J.; Åqvist, J.; Wulff, B. S.; Gutiérrez-de-Terán, H.; Larhammar, D. Elucidation of the Binding Mode of the Carboxyterminal Region of Peptide YY to the Human Y2 Receptor. *Mol. Pharmacol.* **2018**, *93* (4), 323−334.
(108) Keränen, H.; Gutiérrez-de-Terán, H.; Åqvist, J. Structural and Energetic Effects of A2A Adenosine Receptor Mutations on Agonist and Antagonist Binding. *PLoS One* **2014**, *9* (10), No. e108492.
(109) Keränen, H.; Åqvist, J.; Gutiérrez-de-Terán, H. Free Energy Calculations of A2A Adenosine Receptor Mutation Effects on Agonist Binding. *Chem. Commun.* **2015**, *51* (17), 3522−3525.
(110) Jespers, W.; Oliveira, A.; Prieto-Díaz, R.; Majellaro, M.; Åqvist, J.; Sotelo, E.; Gutiérrez-de-Terán, H. Structure-Based Design of Potent and Selective Ligands at the Four Adenosine Receptors. *Molecules* **2017**, *22* (11), 1945.
(111) Nøhr, A. C.; Jespers, W.; Shehata, M. A.; Floryan, L.; Isberg, V.; Andersen, K. B.; Åqvist, J.; Gutiérrez-de-Terán, H.; Bräuner-Osborne, H.; Gloriam, D. E. The GPR139 Reference Agonists 1a and 7c, and Tryptophan and Phenylalanine Share a Common Binding Site. *Sci. Rep* **2017**, *7* (1), 1128.
(112) Chen, D.; Ranganathan, A.; IJzerman, A. P.; Siegal, G.; Carlsson, J. Complementarity between in Silico and Biophysical Screening Approaches in Fragment-Based Lead Discovery against the A2A Adenosine Receptor. *J. Chem. Inf. Model.* **2013**, *53* (10), 2701−2714.
(113) Goldfeld, D. A.; Murphy, R.; Kim, B.; Wang, L.; Beuming, T.; Abel, R.; Friesner, R. A. Docking and Free Energy Perturbation Studies of Ligand Binding in the Kappa Opioid Receptor. *J. Phys. Chem. B* **2015**, *119* (3), 824−835.
(114) Lee, H. S.; Seok, C.; Im, W. Potential Application of Alchemical Free Energy Simulations to Discriminate GPCR Ligand Efficacy. *J. Chem. Theory Comput.* **2015**, *11* (3), 1255−1266.
(115) Panel, N.; Vo, D. D.; Kahlous, N. A.; Hübner, H.; Tiedt, S.; Matricon, P.; Pacalon, J.; Fleetwood, O.; Kampen, S.; Luttens, A.; Delemotte, L.; Kihlberg, J.; Gmeiner, P.; Carlsson, J. Design of Drug Efficacy Guided by Free Energy Simulations of the B2-Adrenoceptor. *Angew. Chem., Int. Ed.* **2023**, *62* (22), No. e202218959.
(116) Matricon, P.; Vo, D. D.; Gao, Z.-G.; Kihlberg, J.; Jacobson, K. A.; Carlsson, J. Fragment-Based Design of Selective GPCR Ligands Guided by Free Energy Simulations. *Chem. Commun.* **2021**, *57* (92), 12305−12308.
(117) Matricon, P.; Ranganathan, A.; Warnick, E.; Gao, Z.-G.; Rudling, A.; Lambertucci, C.; Marucci, G.; Ezzati, A.; Jaiteh, M.; Dal Ben, D.; Jacobson, K. A.; Carlsson, J. Fragment Optimization for GPCRs by Molecular Dynamics Free Energy Calculations: Probing Druggable Subpockets of the A 2A Adenosine Receptor Binding Site. *Sci. Rep* **2017**, *7* (1), 6398.
(118) Dickson, C. J.; Hornak, V.; Duca, J. S. Relative Binding Free-Energy Calculations at Lipid-Exposed Sites: Deciphering Hot Spots. *J. Chem. Inf. Model.* **2021**, *61* (12), 5923−5930.
(119) Wan, S.; Potterton, A.; Husseini, F. S.; Wright, D. W.; Heifetz, A.; Malawski, M.; Townsend-Nicholson, A.; Coveney, P. V. Hit-to-Lead and Lead Optimization Binding Free Energy Calculations for G Protein-Coupled Receptors. *Interface Focus* **2020**, *10* (6), No. 20190128.
(120) Bhati, A. P.; Wan, S.; Wright, D. W.; Coveney, P. V. Rapid, Accurate, Precise, and Reliable Relative Free Energy Prediction Using Ensemble Based Thermodynamic Integration. *J. Chem. Theory Comput* **2017**, *13* (1), 210−222.
(121) Jespers, W.; Verdon, G.; Azuaje, J.; Majellaro, M.; Keränen, H.; García-Mera, X.; Congreve, M.; Deflorian, F.; de Graaf, C.; Zhukov, A.; Doré, A. S.; Mason, J. S.; Åqvist, J.; Cooke, R. M.; Sotelo, E.; Gutiérrez-de-Terán, H. X-Ray Crystallography and Free Energy Calculations Reveal the Binding Mechanism of A2A Adenosine Receptor Antagonists. *Angew. Chem., Int. Ed.* **2020**, *59* (38), 16536−16543.
(122) Cappel, D.; Hall, M. L.; Lenselink, E. B.; Beuming, T.; Qi, J.; Bradner, J.; Sherman, W. Relative Binding Free Energy Calculations

Applied to Protein Homology Models. *J. Chem. Inf. Model.* **2016**, *56* (12), 2388−2400.
(123) Azuaje, J.; Jespers, W.; Yaziji, V.; Mallo, A.; Majellaro, M.; Caamaño, O.; Loza, M. I.; Cadavid, M. I.; Brea, J.; Åqvist, J.; Sotelo, E.; Gutiérrez-de-Terán, H. Effect of Nitrogen Atom Substitution in A3 Adenosine Receptor Binding: N-(4,6-Diarylpyridin-2-Yl)-Acetamides as Potent and Selective Antagonists. *J. Med. Chem.* **2017**, *60* (17), 7502−7511.
(124) Bortolato, A.; Tehan, B. G.; Bodnarchuk, M. S.; Essex, J. W.; Mason, J. S. Water Network Perturbation in Ligand Binding: Adenosine A2A Antagonists as a Case Study. *J. Chem. Inf. Model.* **2013**, *53* (7), 1700−1713.
(125) Jandova, Z.; Jespers, W.; Sotelo, E.; Gutiérrez-de-Terán, H.; Oostenbrink, C. Free-Energy Calculations for Bioisosteric Modifications of A3 Adenosine Receptor Antagonists. *International Journal of Molecular Sciences* **2019**, *20* (14), 3499.
(126) Dalke, A.; Hert, J.; Kramer, C. Mmpdb: An Open-Source Matched Molecular Pair Platform for Large Multiproperty Data Sets. *J. Chem. Inf. Model.* **2018**, *58* (5), 902−910.
(127) Lebon, G.; Warne, T.; Edwards, P. C.; Bennett, K.; Langmead, C. J.; Leslie, A. G. W.; Tate, C. G. Agonist-Bound Adenosine A2A Receptor Structures Reveal Common Features of GPCR Activation. *Nature* **2011**, *474* (7352), 521−525.
(128) Matricon, P.; Suresh, R. R.; Gao, Z.-G.; Panel, N.; Jacobson, K. A.; Carlsson, J. Ligand Design by Targeting a Binding Site Water. *Chem. Sci.* **2021**, *12* (3), 960−968.
(129) Bian, Y.; Xie, X.-Q. (Sean). Computational Fragment-Based Drug Design: Current Trends, Strategies, and Applications. *AAPS J.* **2018**, *20* (3), 59.
(130) Miranda, W. E.; Ngo, V. A.; Perissinotti, L. L.; Noskov, S. Yu. Computational Membrane Biophysics: From Ion Channel Interactions with Drugs to Cellular Function. *Biochimica et Biophysica Acta (BBA) - Proteins and Proteomics* **2017**, *1865* (11), 1643−1653.
(131) Cecchini, M.; Changeux, J.-P. The Nicotinic Acetylcholine Receptor and Its Prokaryotic Homologues: Structure, Conformational Transitions & Allosteric Modulation. *Neuropharmacology* **2015**, *96*, 137−149.
(132) Cecchini, M.; Changeux, J.-P. Nicotinic Receptors: From Protein Allostery to Computational Neuropharmacology. *Molecular Aspects of Medicine* **2022**, *84*, No. 101044.
(133) Liu, L. T.; Willenbring, D.; Xu, Y.; Tang, P. General Anesthetic Binding to Neuronal A4β2 Nicotinic Acetylcholine Receptor and Its Effects on Global Dynamics. *J. Phys. Chem. B* **2009**, *113* (37), 12581−12589.
(134) Liu, L. T.; Haddadian, E. J.; Willenbring, D.; Xu, Y.; Tang, P. Higher Susceptibility to Halothane Modulation in Open- Than in Closed-Channel A4β2 NAChR Revealed by Molecular Dynamics Simulations. *J. Phys. Chem. B* **2010**, *114* (1), 626−632.
(135) LeBard, D. N.; Hénin, J.; Eckenhoff, R. G.; Klein, M. L.; Brannigan, G. General Anesthetics Predicted to Block the GLIC Pore with Micromolar Affinity. *PLOS Computational Biology* **2012**, *8* (5), No. e1002532.
(136) Spurny, R.; Billen, B.; Howard, R. J.; Brams, M.; Debaveye, S.; Price, K. L.; Weston, D. A.; Strelkov, S. V.; Tytgat, J.; Bertrand, S.; Bertrand, D.; Lummis, S. C. R.; Ulens, C. Multisite Binding of a General Anesthetic to the Prokaryotic Pentameric Erwinia Chrysanthemi Ligand-Gated Ion Channel (ELIC) *. *J. Biol. Chem.* **2013**, *288* (12), 8355−8364.
(137) Gkeka, P.; Eleftheratos, S.; Kolocouris, A.; Cournia, Z. Free Energy Calculations Reveal the Origin of Binding Preference for Aminoadamantane Blockers of Influenza A/M2TM Pore. *J. Chem. Theory Comput.* **2013**, *9* (2), 1272−1281.
(138) Ioannidis, H.; Drakopoulos, A.; Tzitzoglaki, C.; Homeyer, N.; Kolarov, F.; Gkeka, P.; Freudenberger, K.; Liolios, C.; Gauglitz, G.; Cournia, Z.; Gohlke, H.; Kolocouris, A. Alchemical Free Energy Calculations and Isothermal Titration Calorimetry Measurements of Aminoadamantanes Bound to the Closed State of Influenza A/M2TM. *J. Chem. Inf. Model.* **2016**, *56* (5), 862−876.
(139) Woll, K. A.; Murlidaran, S.; Pinch, B. J.; Hénin, J.; Wang, X.; Salari, R.; Covarrubias, M.; Dailey, W. P.; Brannigan, G.; Garcia, B. A.; Eckenhoff, R. G. A Novel Bifunctional Alkylphenol Anesthetic Allows Characterization of γ-Aminobutyric Acid, Type A (GABAA), Receptor Subunit Binding Selectivity in Synaptosomes *. *J. Biol. Chem.* **2016**, *291* (39), 20473−20486.
(140) Stouffer, A. L.; Acharya, R.; Salom, D.; Levine, A. S.; Di Costanzo, L.; Soto, C. S.; Tereshko, V.; Nanda, V.; Stayrook, S.; DeGrado, W. F. Structural Basis for the Function and Inhibition of an Influenza Virus Proton Channel. *Nature* **2008**, *451* (7178), 596−599.
(141) Negami, T.; Araki, M.; Okuno, Y.; Terada, T. Calculation of Absolute Binding Free Energies between the HERG Channel and Structurally Diverse Drugs. *Sci. Rep* **2019**, *9* (1), 16586.
(142) Jiang, W.; Zhang, H.; Lin, Y.; Im, W.; Lacroix, J. J.; Luo, Y. L. Binding Free Energies of Piezo1 Channel Agonists at Protein-Membrane Interface. *bioRxiv* **2022**. DOI: 10.1101/2022.06.27.497657.
(143) Rashid, M. H.; Heinzelmann, G.; Kuyucak, S. Calculation of Free Energy Changes Due to Mutations from Alchemical Free Energy Simulations. *J. Theor. Comput. Chem.* **2015**, *14* (03), No. 1550023.
(144) Katz, D.; Sindhikara, D.; DiMattia, M.; Leffler, A. E. Potency-Enhancing Mutations of Gating Modifier Toxins for the Voltage-Gated Sodium Channel NaV1.7 Can Be Predicted Using Accurate Free-Energy Calculations. *Toxins* **2021**, *13* (3), 193.
(145) Lim, V. T.; Geragotelis, A. D.; Lim, N. M.; Freites, J. A.; Tombola, F.; Mobley, D. L.; Tobias, D. J. Insights on Small Molecule Binding to the Hv1 Proton Channel from Free Energy Calculations with Molecular Dynamics Simulations. *Sci. Rep* **2020**, *10* (1), 13587.
(146) Geragotelis, A. D.; Wood, M. L.; Göddeke, H.; Hong, L.; Webster, P. D.; Wong, E. K.; Freites, J. A.; Tombola, F.; Tobias, D. J. Voltage-Dependent Structural Models of the Human Hv1 Proton Channel from Long-Timescale Molecular Dynamics Simulations. *Proc. Natl. Acad. Sci. U. S. A.* **2020**, *117* (24), 13490−13498.
(147) Drakopoulos, A.; Tzitzoglaki, C.; Ma, C.; Freudenberger, K.; Hoffmann, A.; Hu, Y.; Gauglitz, G.; Schmidtke, M.; Wang, J.; Kolocouris, A. Affinity of Rimantadine Enantiomers against Influenza A/M2 Protein Revisited. *ACS Med. Chem. Lett.* **2017**, *8* (2), 145−150.
(148) Thomaston, J. L.; Samways, M. L.; Konstantinidi, A.; Ma, C.; Hu, Y.; Bruce Macdonald, H. E.; Wang, J.; Essex, J. W.; DeGrado, W. F.; Kolocouris, A. Rimantadine Binds to and Inhibits the Influenza A M2 Proton Channel without Enantiomeric Specificity. *Biochemistry* **2021**, *60* (32), 2471−2482.
(149) Garaev, T. M.; Odnovorov, A. I.; Lashkov, A. A.; Grebennikova, T. V.; Finogenova, M. P.; Sadykova, G. K.; Prilipov, A. G.; Timofeeva, T. A.; Rubinsky, S. V.; Norkina, S. N.; Zhuravleva, M. M. Studying the Effect of Amino Acid Substitutions in the M2 Ion Channel of the Influenza Virus on the Antiviral Activity of the Aminoadamantane Derivative In Vitro and In Silico. *Adv. Pharm. Bull.* **2021**, *11* (4), 700−711.
(150) Stock, L.; Hosoume, J.; Treptow, W. Concentration-Dependent Binding of Small Ligands to Multiple Saturable Sites in Membrane Proteins. *Sci. Rep* **2017**, *7* (1), 5734.
(151) Stock, L.; Hosoume, J.; Cirqueira, L.; Treptow, W. Binding of the General Anesthetic Sevoflurane to Ion Channels. *PLOS Computational Biology* **2018**, *14* (11), No. e1006605.
(152) Ariz-Extreme, I.; Hub, J. S. Assigning Crystallographic Electron Densities with Free Energy Calculations—The Case of the Fluoride Channel Fluc. *PLoS One* **2018**, *13* (5), No. e0196751.
(153) Wen, P.-C.; Mahinthichaichan, P.; Trebesch, N.; Jiang, T.; Zhao, Z.; Shinn, E.; Wang, Y.; Shekhar, M.; Kapoor, K.; Chan, C. K.; Tajkhorshid, E. Microscopic View of Lipids and Their Diverse Biological Functions. *Curr. Opin Struct Biol.* **2018**, *51*, 177−186.
(154) Corradi, V.; Sejdiu, B. I.; Mesa-Galloso, H.; Abdizadeh, H.; Noskov, S. Yu.; Marrink, S. J.; Tieleman, D. P. Emerging Diversity in Lipid−Protein Interactions. *Chem. Rev.* **2019**, *119* (9), 5775−5848.
(155) Duncan, A. L.; Song, W.; Sansom, M. S. P. Lipid-Dependent Regulation of Ion Channels and G Protein−Coupled Receptors: Insights from Structures and Simulations. *Annual Review of Pharmacology and Toxicology* **2020**, *60* (1), 31−50.

(156) Bushell, S. R.; Pike, A. C. W.; Falzone, M. E.; Rorsman, N. J. G.; Ta, C. M.; Corey, R. A.; Newport, T. D.; Christianson, J. C.; Scofano, L. F.; Shintre, C. A.; Tessitore, A.; Chu, A.; Wang, Q.; Shrestha, L.; Mukhopadhyay, S. M. M.; Love, J. D.; Burgess-Brown, N. A.; Sitsapesan, R.; Stansfeld, P. J.; Huiskonen, J. T.; Tammaro, P.; Accardi, A.; Carpenter, E. P. The Structural Basis of Lipid Scrambling and Inactivation in the Endoplasmic Reticulum Scramblase TMEM16K. *Nat. Commun.* **2019**, *10*, 3956.
(157) Caffalette, C. A.; Corey, R. A.; Sansom, M. S. P.; Stansfeld, P. J.; Zimmer, J. A Lipid Gating Mechanism for the Channel-Forming O Antigen ABC Transporter. *Nat. Commun.* **2019**, *10*, 824.
(158) Rodríguez, Y.; Mezei, M.; Osman, R. Association Free Energy of Dipalmitoylphosphatidylserines in a Mixed Dipalmitoylphosphatidylcholine Membrane. *Biophys. J.* **2007**, *92* (9), 3071−3080.
(159) Simonson, T.; Archontis, G.; Karplus, M. Continuum Treatment of Long-Range Interactions in Free Energy Calculations. Application to Protein−Ligand Binding. *J. Phys. Chem. B* **1997**, *101* (41), 8349−8362.
(160) Tidor, B.; Karplus, M. Simulation Analysis of the Stability Mutant R96H of T4 Lysozyme. *Biochemistry* **1991**, *30* (13), 3217−3228.
(161) Rodríguez, Y.; Mezei, M.; Osman, R. The PT1−Ca2+ Gla Domain Binds to a Membrane through Two Dipalmitoylphosphatidylserines. A Computational Study. *Biochemistry* **2008**, *47* (50), 13267−13278.
(162) Souza, P. C. T.; Alessandri, R.; Barnoud, J.; Thallmair, S.; Faustino, I.; Grünewald, F.; Patmanidis, I.; Abdizadeh, H.; Bruininks, B. M. H.; Wassenaar, T. A.; Kroon, P. C.; Melcr, J.; Nieto, V.; Corradi, V.; Khan, H. M.; Domański, J.; Javanainen, M.; Martinez-Seara, H.; Reuter, N.; Best, R. B.; Vattulainen, I.; Monticelli, L.; Periole, X.; Tieleman, D. P.; de Vries, A. H.; Marrink, S. J. Martini 3: A General Purpose Force Field for Coarse-Grained Molecular Dynamics. *Nat. Methods* **2021**, *18* (4), 382−388.
(163) Fathizadeh, A.; Senning, E.; Elber, R. Impact of the Protonation State of Phosphatidylinositol 4,5-Bisphosphate (PIP2) on the Binding Kinetics and Thermodynamics to Transient Receptor Potential Vanilloid (TRPV5): A Milestoning Study. *J. Phys. Chem. B* **2021**, *125* (33), 9547−9556.
(164) Larsen, A. H.; Tata, L.; John, L. H.; Sansom, M. S. P. Membrane-Binding Mechanism of the EEA1 FYVE Domain Revealed by Multi-Scale Molecular Dynamics Simulations. *PLOS Computational Biology* **2021**, *17* (9), No. e1008807.
(165) Larsen, A. H.; Sansom, M. S. P. Binding of Ca2+-Independent C2 Domains to Lipid Membranes: A Multi-Scale Molecular Dynamics Study. *Structure* **2021**, *29* (10), 1200−1213.e2.
(166) Wang, Q.; Corey, R. A.; Hedger, G.; Aryal, P.; Grieben, M.; Nasrallah, C.; Baronina, A.; Pike, A. C. W.; Shi, J.; Carpenter, E. P.; Sansom, M. S. P. Lipid Interactions of a Ciliary Membrane TRP Channel: Simulation and Structural Studies of Polycystin-2. *Structure* **2020**, *28* (2), 169−184.e5.
(167) Larsen, A. H.; John, L. H.; Sansom, M. S. P.; Corey, R. A. Specific Interactions of Peripheral Membrane Proteins with Lipids: What Can Molecular Simulations Show Us. *Biosci Rep* **2022**, *42* (4), No. BSR20211406.
(168) Pipatpolkai, T.; Corey, R. A.; Proks, P.; Ashcroft, F. M.; Stansfeld, P. J. Evaluating Inositol Phospholipid Interactions with Inward Rectifier Potassium Channels and Characterising Their Role in Disease. *Commun. Chem.* **2020**, *3* (1), 1−10.
(169) Panasawatwong, A.; Pipatpolkai, T.; Tucker, S. J. Transition between Conformational States of the TREK-1 K2P Channel Promoted by Interaction with PIP2. *Biophys. J.* **2022**, *121* (12), 2380−2388.
(170) Duncan, A. L.; Corey, R. A.; Sansom, M. S. P. Defining How Multiple Lipid Species Interact with Inward Rectifier Potassium (Kir2) Channels. *Proc. Natl. Acad. Sci. U. S. A.* **2020**, *117* (14), 7803−7813.
(171) Corey, R. A.; Harrison, N.; Stansfeld, P. J.; Sansom, M. S. P.; Duncan, A. L. Cardiolipin, and Not Monolysocardiolipin, Preferentially Binds to the Interface of Complexes III and IV. *Chem. Sci.* **2022**, *13* (45), 13489−13498.
(172) Miranda, W. E.; Guo, J.; Mesa-Galloso, H.; Corradi, V.; Lees-Miller, J. P.; Tieleman, D. P.; Duff, H. J.; Noskov, S. Y. Lipid Regulation of HERG1 Channel Function. *Nat. Commun.* **2021**, *12* (1), 1409.
(173) Phillips, J. C.; Braun, R.; Wang, W.; Gumbart, J.; Tajkhorshid, E.; Villa, E.; Chipot, C.; Skeel, R. D.; Kalé, L.; Schulten, K. Scalable Molecular Dynamics with NAMD. *J. Comput. Chem.* **2005**, *26* (16), 1781−1802.
(174) Waheed, Q.; Khan, H. M.; He, T.; Roberts, M.; Gershenson, A.; Reuter, N. Interfacial Aromatics Mediating Cation−π Interactions with Choline-Containing Lipids Can Contribute as Much to Peripheral Protein Affinity for Membranes as Aromatics Inserted below the Phosphates. *J. Phys. Chem. Lett.* **2019**, *10* (14), 3972−3977.
(175) Roberts, M. F.; Gershenson, A.; Reuter, N. Phosphatidylcholine Cation—Tyrosine π Complexes: Motifs for Membrane Binding by a Bacterial Phospholipase C. *Molecules* **2022**, *27* (19), 6184.
(176) Yoo, J.; Cui, Q. Does Arginine Remain Protonated in the Lipid Membrane? Insights from Microscopic PKa Calculations. *Biophys. J.* **2008**, *94* (8), L61−L63.
(177) Yoo, J.; Cui, Q. Chemical versus Mechanical Perturbations on the Protonation State of Arginine in Complex Lipid Membranes: Insights from Microscopic PKa Calculations. *Biophys. J.* **2010**, *99* (5), 1529−1538.
(178) Sengupta, D. Cholesterol Modulates the Structure, Binding Modes, and Energetics of Caveolin−Membrane Interactions. *J. Phys. Chem. B* **2012**, *116* (50), 14556−14564.
(179) Zhang, L.; Yethiraj, A.; Cui, Q. Free Energy Calculations for the Peripheral Binding of Proteins/Peptides to an Anionic Membrane. 1. Implicit Membrane Models. *J. Chem. Theory Comput.* **2014**, *10* (7), 2845−2859.
(180) Schäfer, L. V.; de Jong, D. H.; Holt, A.; Rzepiela, A. J.; de Vries, A. H.; Poolman, B.; Killian, J. A.; Marrink, S. J. Lipid Packing Drives the Segregation of Transmembrane Helices into Disordered Lipid Domains in Model Membranes. *Proc. Natl. Acad. Sci. U. S. A.* **2011**, *108* (4), 1343−1348.
(181) Brewer, A.; Zhang, L. Binding Free Energy Calculation of Human Beta Defensin 3 with Negatively Charged Lipid Bilayer Using Free Energy Perturbation Method. *Biophys. Chem.* **2021**, *277*, No. 106662.
(182) Gumbart, J.; Chipot, C.; Schulten, K. Free-Energy Cost for Translocon-Assisted Insertion of Membrane Proteins. *Proc. Natl. Acad. Sci. U. S. A.* **2011**, *108* (9), 3596−3601.
(183) Gumbart, J.; Roux, B. Determination of Membrane-Insertion Free Energies by Molecular Dynamics Simulations. *Biophys. J.* **2012**, *102* (4), 795−801.
(184) Dubey, V.; Prasanna, X.; Sengupta, D. Estimating the Lipophobic Contributions in Model Membranes. *J. Phys. Chem. B* **2017**, *121* (9), 2111−2120.
(185) Dar, D. E.; Metzger, T. G.; Vandenbergh, D. J.; Uhl, G. R. Dopamine Uptake and Cocaine Binding Mechanisms: The Involvement of Charged Amino Acids from the Transmembrane Domains of the Human Dopamine Transporter. *Eur. J. Pharmacol.* **2006**, *538* (1), 43−47.
(186) Jacobsen, L.; Husen, P.; Solov'yov, I. A. Inhibition Mechanism of Antimalarial Drugs Targeting the Cytochrome Bc1 Complex. *J. Chem. Inf. Model.* **2021**, *61* (3), 1334−1345.
(187) Warnau, J.; Wöhlert, D.; Okazaki, K.; Yildiz, Ö.; Gamiz-Hernandez, A. P.; Kaila, V. R. I.; Kühlbrandt, W.; Hummer, G. Ion Binding and Selectivity of the Na+/H+ Antiporter MjNhaP1 from Experiment and Simulation. *J. Phys. Chem. B* **2020**, *124* (2), 336−344.
(188) Abramyan, A. M.; Slack, R. D.; Meena, S.; Davis, B. A.; Newman, A. H.; Singh, S. K.; Shi, L. Computation-Guided Analysis of Paroxetine Binding to HSERT Reveals Functionally Important Structural Elements and Dynamics. *Neuropharmacology* **2019**, *161*, No. 107411.
(189) Salomon, K.; Abramyan, A.; Plenge, P.; Wang, L.; Bang-Andersen, B.; Loland, C.; Shi, L. Dynamic Extracellular Vestibule of

https://doi.org/10.1021/acs.jctc.3c00365
J. Chem. Theory Comput. 2023, 19, 7437−7458

Human SERT: Unveiling Druggable Potential with Novel High-Affinity Allosteric Inhibitors; *ChemRxiv* **2023**. DOI: 10.26434/chemrxiv-2023-wcjnt.
(190) Maynard, J. A.; Lindquist, N. C.; Sutherland, J. N.; Lesuffleur, A.; Warrington, A. E.; Rodriguez, M.; Oh, S.-H. Next Generation SPR Technology of Membrane-Bound Proteins for Ligand Screening and Biomarker Discovery. *Biotechnol J.* **2009**, *4* (11), 1542−1558.
(191) Patching, S. G. Surface Plasmon Resonance Spectroscopy for Characterisation of Membrane Protein−Ligand Interactions and Its Potential for Drug Discovery. *Biochimica et Biophysica Acta (BBA) - Biomembranes* **2014**, *1838* (1), 43−55.
(192) Capelli, D.; Parravicini, C.; Pochetti, G.; Montanari, R.; Temporini, C.; Rabuffetti, M.; Trincavelli, M. L.; Daniele, S.; Fumagalli, M.; Saporiti, S.; Bonfanti, E.; Abbracchio, M. P.; Eberini, I.; Ceruti, S.; Calleri, E.; Capaldi, S. Surface Plasmon Resonance as a Tool for Ligand Binding Investigation of Engineered GPR17 Receptor, a G Protein Coupled Receptor Involved in Myelination. *Front. Chem.* **2020**, *7*. DOI: 10.3389/fchem.2019.00910
(193) He, J.; Haney, R. M.; Vora, M.; Verkhusha, V. V.; Stahelin, R. V.; Kutateladze, T. G. Molecular Mechanism of Membrane Targeting by the GRP1 PH Domain *s. *J. Lipid Res.* **2008**, *49* (8), 1807−1815.
(194) Lamour, N. F.; Subramanian, P.; Wijesinghe, D. S.; Stahelin, R. V.; Bonventre, J. V.; Chalfant, C. E. Ceramide 1-Phosphate Is Required for the Translocation of Group IVA Cytosolic Phospholipase A2 and Prostaglandin Synthesis *. *J. Biol. Chem.* **2009**, *284* (39), 26897−26907.
(195) Heller, B.; Adu-Gyamfi, E.; Smith-Kinnaman, W.; Babbey, C.; Vora, M.; Xue, Y.; Bittman, R.; Stahelin, R. V.; Wells, C. D. Amot Recognizes a Juxtanuclear Endocytic Recycling Compartment via a Novel Lipid Binding Domain *. *J. Biol. Chem.* **2010**, *285* (16), 12308−12320.
(196) Gil, J.-E.; Kim, E.; Kim, I.-S.; Ku, B.; Park, W. S.; Oh, B.-H.; Ryu, S. H.; Cho, W.; Heo, W. D. Phosphoinositides Differentially Regulate Protrudin Localization through the FYVE Domain *. *J. Biol. Chem.* **2012**, *287* (49), 41268−41276.
(197) Ferguson, K. M.; Kavran, J. M.; Sankaran, V. G.; Fournier, E.; Isakoff, S. J.; Skolnik, E. Y.; Lemmon, M. A. Structural Basis for Discrimination of 3-Phosphoinositides by Pleckstrin Homology Domains. *Mol. Cell* **2000**, *6* (2), 373−384.
(198) Klarlund, J. K.; Tsiaras, W.; Holik, J. J.; Chawla, A.; Czech, M. P. Distinct Polyphosphoinositide Binding Selectivities for Pleckstrin Homology Domains of GRP1-like Proteins Based on DiglycineVersus Triglycine Motifs *. *J. Biol. Chem.* **2000**, *275* (42), 32816−32821.
(199) Cherezov, V. Lipidic Cubic Phase Technologies for Membrane Protein Structural Studies. *Curr. Opin Struct Biol.* **2011**, *21* (4), 559−566.
(200) Gater, D. L.; Saurel, O.; Iordanov, I.; Liu, W.; Cherezov, V.; Milon, A. Two Classes of Cholesterol Binding Sites for the B2AR Revealed by Thermostability and NMR. *Biophys. J.* **2014**, *107* (10), 2305−2312.
(201) Laganowsky, A.; Reading, E.; Allison, T. M.; Ulmschneider, M. B.; Degiacomi, M. T.; Baldwin, A. J.; Robinson, C. V. Membrane Proteins Bind Lipids Selectively to Modulate Their Structure and Function. *Nature* **2014**, *510* (7503), 172−175.
(202) Gault, J.; Liko, I.; Landreh, M.; Shutin, D.; Bolla, J. R.; Jefferies, D.; Agasid, M.; Yen, H.-Y.; Ladds, M. J. G. W.; Lane, D. P.; Khalid, S.; Mullen, C.; Remes, P. M.; Huguet, R.; McAlister, G.; Goodwin, M.; Viner, R.; Syka, J. E. P.; Robinson, C. V. Combining Native and 'Omics' Mass Spectrometry to Identify Endogenous Ligands Bound to Membrane Proteins. *Nat. Methods* **2020**, *17* (5), 505−508.
(203) *Drug Design: Structure- and Ligand-Based Approaches*; Merz, K. M., Ringe, D., Reynolds, C. H., Eds.; Cambridge University Press: Cambridge [U.K.]; New York, 2010.
(204) Abel, R.; Wang, L.; Mobley, D. L.; Friesner, R. A. A Critical Review of Validation, Blind Testing, and Real- World Use of Alchemical Protein-Ligand Binding Free Energy Calculations. *Current topics in medicinal chemistry* **2017**, *17* (23), 2577−2585.
(205) Tresadern, G.; Tatikola, K.; Cabrera, J.; Wang, L.; Abel, R.; van Vlijmen, H.; Geys, H. The Impact of Experimental and Calculated Error on the Performance of Affinity Predictions. *J. Chem. Inf. Model.* **2022**, *62* (3), 703−717.
(206) Lu, J.; Byrne, N.; Wang, J.; Bricogne, G.; Brown, F. K.; Chobanian, H. R.; Colletti, S. L.; Di Salvo, J.; Thomas-Fowlkes, B.; Guo, Y.; Hall, D. L.; Hadix, J.; Hastings, N. B.; Hermes, J. D.; Ho, T.; Howard, A. D.; Josien, H.; Kornienko, M.; Lumb, K. J.; Miller, M. W.; Patel, S. B.; Pio, B.; Plummer, C. W.; Sherborne, B. S.; Sheth, P.; Souza, S.; Tummala, S.; Vonrhein, C.; Webb, M.; Allen, S. J.; Johnston, J. M.; Weinglass, A. B.; Sharma, S.; Soisson, S. M. Structural Basis for the Cooperative Allosteric Activation of the Free Fatty Acid Receptor GPR40. *Nat. Struct Mol. Biol.* **2017**, *24* (7), 570−577.
(207) Doré, A. S.; Okrasa, K.; Patel, J. C.; Serrano-Vega, M.; Bennett, K.; Cooke, R. M.; Errey, J. C.; Jazayeri, A.; Khan, S.; Tehan, B.; Weir, M.; Wiggin, G. R.; Marshall, F. H. Structure of Class C GPCR Metabotropic Glutamate Receptor 5 Transmembrane Domain. *Nature* **2014**, *511* (7511), 557−562.
(208) Jazayeri, A.; Rappas, M.; Brown, A. J. H.; Kean, J.; Errey, J. C.; Robertson, N. J.; Fiez-Vandal, C.; Andrews, S. P.; Congreve, M.; Bortolato, A.; Mason, J. S.; Baig, A. H.; Teobald, I.; Doré, A. S.; Weir, M.; Cooke, R. M.; Marshall, F. H. Crystal Structure of the GLP-1 Receptor Bound to a Peptide Agonist. *Nature* **2017**, *546* (7657), 254−258.
(209) Gharpure, A.; Noviello, C. M.; Hibbs, R. E. Progress in Nicotinic Receptor Structural Biology. *Neuropharmacology* **2020**, *171*, No. 108086.